NASA CR-134699

BCAC D6-41908

THE RESULTS OF A LOW-SPEED WIND TUNNEL TEST TO INVESTIGATE THE EFFECTS OF THE REFAN JT8D ENGINE TARGET THRUST REVERSER ON THE STABILITY AND CONTROL CHARACTERISTICS OF THE BOEING 727-200 AIRPLANE

by E. A. Kupcis

BOEING COMMERCIAL AIRPLANE COMPANY

A DIVISION OF

THE BOEING COMPANY

Prepared for

NATIONAL AERONAUTICS AND SPACE ADMINISTRATION

NASA Lewis Research Center

Contract NAS3-17842

FOREWORD

The low-speed wind tunnel test described in this report was performed by the Flight Controls Technology Staff of The Boeing Commercial Airplane Company, a division of The Boeing Company, Seattle, Washington. The work, sponsored by NASA Lewis Research Center and reported herein, was performed in April 1974.

This report has been reviewed and is approved by:

J.C. Hall Date 9·16·74

F. C. Hall, Group Engineer
Flight Controls Technology Staff

J. A Ferrell Date 9-16-74

J. A Ferrell
Chief, Staff Technology
JT8D Refan Program

K P Rice Date 9/16/74

K. P. Rice
Program Manager
JT8D Refan Program

TABLE OF CONTENTS

1.0 SUMMARY

A low-speed, powered, wind tunnel model of the Boeing 727-200 airplane was tested in support of the NASA Refan Program. The purpose of the test was to investigate the effects of the Refan side engine target thrust reverser configuration on airplane directional control characteristics during the landing rollout.

The following conclusions are made:

1. The Refan airplane, with its target thrust reverser configuration, exhibits slightly improved directional control characteristics relative to those of the Basic 727 airplane.

2. Clocking the Refan side engine thrust reversers 20 degrees outboard, to direct the reverser efflux away from the vertical tail, has only a minor effect on directional control.

3. Clocking the Refan thrust reversers 20 degrees inboard, directing the reverser efflux toward the vertical tail, results in a virtual loss of rudder effectiv ess for speeds above 90 knots (46.4 m/sec). This is not considered an acceptable configuration, since the rudder is the primary means of directional control during the high speed segment of the landing rollout.

4. Variations in the Refan reverser door lip/fence geometry produce only minor changes in airplane directional control characteristics.

5. Refan airplane asymmetric reverse thrust characteristics are not unusual.

2.0 INTRODUCTION

The Pratt and Whitney aircraft JT8D-100 series Refan engine is a derivative of the basic JT8D turbofan engine, modified to incorporate a new, larger diameter, single-stage fan with a bypass ratio of 2.0 and two supercharging, low-pressure compressor stages. The modification gives lower jet noise, increased takeoff and cruise thrust, and lower specific fuel consumption The Boeing 727 airplane, equipped with the JT8D-100 series engine, and incorporating a target type thrust reverser, is referred to as the Refan configuration. The production 727 airplane, equipped with the basic JT8D engine, and incorporating the production clamshell-deflector door thrust reverser, is referred to as the Basic configuration.

The thrust reverser installation on the 727 airplane is used to assist airplane deceleration during the landing rollout. It is designed for ground operation only. The reversers are particularly beneficial during landings on slippery runways where wheel braking efficiency is reduced.

For airplane configurations such as the 727, where the engines are mounted in close proximity to the vertical tail, thrust reverser operation can result in reduced vertical tail and rudder effectiveness. The thrust reverser jet efflux mixes with the free-stream flow, reducing the dynamic pressure at the vertical tail. Some areas of the tail may actually experience flow separation due to direct impingement of the reverse thrust flow. The combined phenomena result in the so-called "tail blanking" effect.

Reduced rudder effectiveness during the landing rollout, particularly under crosswind and slippery runway conditions, can lead to operational restrictions such as reduced crosswind landing limits or limitations on the use of reverse thrust.

The degree of "tail blanking" is a function of engine thrust, airspeed, and sideslip angle, and is strongly dependent on the thrust reverser geometry and its relative proximity to the vertical tail and rudder. The geometric differences between the Refan and Basic airplane thrust reverser installations, and the higher thrust and mass flow of the Refan engine, as well as its more effective thrust reverser design, will result in different "tail blanking" characteristics.

Due to the complex nature of the "tail blanking" phenomena, and the inadequacy of analytical prediction methods, wind tunnel testing is required to determine the effect of the Refan target thrust reverser on airplane directional control characteristics.

A low-speed wind tunnel test, utilizing a powered scale model of the Refan 727-200 airplane, was conducted at the Boeing-Vertol 20 x 20 ft (6.10 x 6.10 m) Low-Speed Wind Tunnel at Philadelphia, Pa., in April 1974. Thrust reversers were installed on the two side-mounted engines only. The Basic 727 airplane thrust reverser installation was also evaluated to provide a baseline for comparison. In addition, Refan thrust reverser clock angle (reverser door angle, in the rear view, with respect to the vertical) and lip/fence geometry variations were tested, in the event they may be required in the final T/R design to improve "tail blanking" and/or engine re-ingestion characteristics.

The effect of the Refan engine target thrust reverser on the directional control characteristics of the 727-200 airplane, as determined from the Vertol test, is the subject of this report. The data are intended to provide incremental information between the Refan and Basic reverser configurations, as well as effects of clocking and lip/fence geometry changes. As such, they should not be used to calculate absolute performance levels for either configuration.

3.0 NOMENCLATURE

b	Wing span
$\bar{c}$	Mean aerodynamic chord of the wing
C_μ	Thrust coefficient, F_G/qS_W
C_N	Yawing moment coefficient about the MAC/4, yawing moment/qS_Wb, positive airplane nose right
C_Y	Side force coefficient, side force/qS_W, positive right
C_l	Rolling moment coefficient, rolling moment/qS_Wb, positive right wing down
$\Delta C_{N_{@\ \beta=15°}}$	Yawing moment coefficient at β = 15 deg.
$C_{N_{\delta R}}$	Yawing moment coefficient per degree of rudder deflection (δ_R)
EPR	Full scale engine pressure ratio, exit total pressure/inlet total pressure
F_G	Gross thrust, lbs.
h	Height of wing MAC/4 above ground plane
MAC/4	Wing quarter chord
N/m^2	Pressure in Newtons per square meter
q	Free stream dynamic pressure, lbs/ft^2, $V_E^2/295$
S_W	Wing reference area, ft^2
T/R	Thrust reverser
V_E	Equivalent airspeed, knots
α_{BODY}	Body angle of attack, degrees
β	Angle of sideslip, degrees, positive for wind from right
δ_R	Rudder deflection, degrees, positive trailing edge left
$\theta_{T/R}$	Refan thrust reverser clock angle, degrees, see Page 40 Figure 18 for definition

4.0 MODEL AND TEST DESCRIPTION

4.1 MODEL DESCRIPTION

4.1.1 BASIC MODEL

The model, designated TX-549 I-3, is a 7.5 percent scale model of the Boeing 727-200 airplane. A three-view drawing of the Refan configuration indicating the major dimensions is shown in Figure 1. The model was sting mounted with an internal, six-component, strain-gauge balance for measuring forces and moments. It was flown in the landing configuration, at taxi attitude, over a moving belt ground plane. The two blowing side nacelles were mounted directly on the sting strut to isolate them from the main balance. In this manner, only the aerodynamic interference effects due to blowing were recorded on the balance. The compressed air for engine blowing was supplied through the string strut mount.

Both the Refan and the Basic 727 configurations, with their respective thrust reverser designs, were tested. The model installation is shown in Figure 2. Closeups of the blowing Refan side nacelle, with the thrust reverser stowed and in the deployed positions, are shown in Figures 3 and 4 respectively.

4.1.2 NACELLE AND THRUST REVERSER GEOMETRY

The blowing side nacelles were scaled to simulate the Refan engine. The nacelle exits were removable so that the nacelles could be tested with both a clean nozzle and with the thrust reverser deployed. The Basic configuration was simulated at the nacelle exit only by using the appropriate exit nozzle diameter and thrust reverser configuration.

The Refan airplane utilizes a target type thrust reverser, whereas the Basic has a clamshell-deflector door design. The model parts simulating these thrust reverser configurations, as well as the clean exit nozzles, are shown in Figure 5.

The blown side nacelles are of the plugged inlet type (Figures 3 and 4) with a plenum chamber at the forward end, two choke plates to give the correct thrust-exit pressure relationship, and a pressure and temperature measuring rake at the aft end to provide inputs for thrust parameter setting and calculation.

The sting mount precluded the use of a blown center engine. This was considered to be an acceptable compromise since the effect of center engine reverse thrust is secondary. In addition, the center engine inlets were plugged for both the Refan and Basic configurations.

4.2 TEST FACILITY AND MODEL INSTALLATION

The test was conducted at the Boeing-Vertol Low Speed Wind Tunnel in Philadelphia, Pa. The test facility has a 20 x 20 foot (6.10 x 6.10 meter) test section, which is vented to the atmosphere. Ground plane simulation is enhanced by the use of a moving belt ground plane which is capable of speeds up to 100 knots (51.4 m/sec). In addition, compressed air is available for blowing models at a maximum rate of 20 lb/sec. (9.08 KG/Sec) at 1000 PSI (6.883×10^6 N/M^2).

The model was installed on the Boeing 635H, six-component, internal strain gauge balance. The sting strut mount was used to duct high pressure air to the model. The blowing side nacelles were mounted directly to the strut and physically separated from the rest of the model. In this way only aerodynamic

loads, excluding those on the nacelles and reversers, were measured by the wind tunnel balance. Comparison with previous wind tunnel test data indicates that the exclusion of the nacelle and reverser aerodynamic loads does not significantly alter the test results.

4.3 THRUST SIMULATION AND CALIBRATION

The full scale engine was simulated by scaling the nozzle exit and thrust reverser geometry, and by matching the full scale thrust coefficient C_μ. The thrust coefficient is defined as:

$$C_\mu = F_G/qS_W$$

where F_G = Gross thrust - lb.

q = Free-stream dynamic pressure - PSF

S_W = Wing reference area - ft^2.

The engine exhaust flow was simulated by using cold compressed air. The individual fan and primary air flows of the full scale engine were not simulated, but rather the mixed flow. As the nacelle inlets were plugged, inlet flow simulation was not provided.

A thrust calibration of the blown nacelles was conducted prior to the wind tunnel test. All four nozzle exit configurations (Figure 5), for both the left and right nacelles, were calibrated on the thrust stand at Boeing Field, Seattle.

For a fixed nozzle diameter and plenum pressure, the nacelle exit pressure ratio is a function of the exit configuration (reverser stowed or deployed). However, the plenum pressure ratio (referenced to ambient static pressure) for a fixed nozzle diameter, does not vary with exit geometry. For this

reason, the plenum pressure ratio was used as a reference to set thrust on the model.

A summary of the thrust calibration data for the Refan and Basic clean nozzle exits is shown in Figure 6. Full scale engine pressure ratio (EPR) is plotted versus scaled model gross thrust and model plenum pressure ratio. The thrust calibration curves are different for the left and right engines due to small differences in nacelle choke plate geometry between the left and right nacelles.

The 727 airplane reverse thrust is actuated by reverse thrust levers mounted on the engine throttles. A spring detent is incorporated in the system so that a fixed reverse thrust can be selected quickly without having to monitor engine EPR. The reverse thrust spring detent location on the Basic airplane was selected to provide maximum take-off EPR (1.985) on a 0^{o}F day. For higher temperatures the spring detent EPR decreases according to the basic engine thrust-temperature lapse rate. The same design is incorporated on the Refan engine.

Three basic thrust settings were chosen for the test: a maximum take-off EPR thrust, a thrust corresponding to the standard day, 59^{o}F, spring detent EPR, and 50 percent of take-off thrust. The spring detent characteristics and the full scale EPR test conditions are defined in Figure 7 for both the Refan and Basic airplanes.

4.4 TEST PROCEDURE

The model was yawed in ground effect ($\frac{h}{b}$ = .093) in taxi attitude (α_{BODY} = 0 degrees) with the engines at constant EPR (thrust) for airspeeds ranging from 50 to 130 knots (25.7 to 66.9 m/sec). The sideslip range was -5 degrees to +25 degrees. The moving belt ground plane was limited to a maximum speed

of 100 knots (51.5 m/sec). For each EPR/airspeed combination, both the zero rudder and maximum rudder configurations were evaluated.

The Refan and Basic configurations were compared at EPR settings of 1.0 (power off), maximum EPR, 59°F detent EPR, and 50% thrust EPR, as defined in Figure 7. Effects of the Refan thrust reverser clock angle, lip and fence configuration, as well as asymmetric reverse thrust characteristics, were evaluated only at maximum EPR. In addition, each thrust reverser configuration was run at maximum EPR with the tunnel velocity at zero in order to confirm that induced thrust asymmetry forces are small.

Unless otherwise noted, all data shown are for the thrust reversers deployed, and in the case of the Refan reverser, using the project 3.5 inch (8.89 cm) constant chord lip configuration with the doors at zero clock angle.

Flow visualization tuft runs, comparing the Refan and Basic configurations, were also made in order to determine the extent of reverse thrust impingement on the vertical tail and rudder.

Six-component force and moment data were recorded and standard wind tunnel corrections applied.

5.0 DISCUSSION OF TEST RESULTS

5.1 REFAN-BASIC AIRPLANE COMPARISON

5.1.1 RUDDER EFFECTIVENESS AND YAWING MOMENT DUE TO SIDESLIP

Lateral-directional stability and control characteristics during reverse thrust operation are compared for the Refan and Basic airplane thrust reverser configurations in Figures 8 through 13.

Rudder effectiveness ($C_{N_{\delta R}}$) is shown as a function of airspeed and EPR for β = 0 and 15 degrees in Figures 8 and 9, respectively. General data trends for both the Refan and Basic configurations indicate a decreasing rudder effectiveness with decreasing airspeed and increasing EPR (thrust). At the low airspeeds, the dynamic pressure reduction at the vertical tail due to reverse thrust is a relatively larger percentage of the tunnel free-stream dynamic pressure (q) than at higher airspeeds. In addition, the lower tunnel q allows greater spreading and forward penetration of the reverse thrust jet efflux, resulting in more effective "tail blanking". Consequently, the reduction in rudder effectiveness at low speeds is relatively greater. It is also apparent that the higher the EPR setting, the greater the q reduction and degree of "tail blanking", and consequently the larger is the loss in rudder effectiveness.

A comparison of the Refan and Basic configurations indicates that the Refan airplane rudder effectiveness, over the major part of the speed range investigated, is equal to or slightly better than that of the Basic airplane. This is true both for small and large airplane sideslip angles, and is

primarily due to the more favorable aft location of the Refan target reverser. As indicated by a tuft flow visualization study (Sect. 5.1.2), a more aft thrust reverser location results in less forward penetration of the reverser efflux and consequently reduced "tail blanking".

Airplane yawing moment at 15 degrees of sideslip is shown in Figure 10 for both the Refan and Basic airplanes. The comparison is given as a function of airspeed and EPR. The data are for a zero rudder deflection and represent the yawing moment that would have to be trimmed out by the rudder during a typical crosswind landing (15-20 kt. (7.7 - 10.3 m/sec) crosswind component). In general, the data indicate that the Refan configuration has a smaller unbalanced yawing moment than the Basic airplane and thus would require less rudder control during a crosswind landing rollout with reversers operating.

The combination of greater rudder effectiveness and smaller yawing moment due to sideslip will result in improved crosswind landing directional control characteristics for the Refan airplane.

Typical test data showing C_N, C_Y and C_l plotted versus sideslip angle are shown in Figures 11, 12 and 13, respectively. The Refan and Basic configurations are compared at the 110 knot (56.6 m/sec), 59°F detent EPR condition, for zero and maximum rudder.

The yawing moment data (Figure 11) clearly illustrate the improved rudder capability of the Refan airplane. It is also noted that the yawing moment due to sideslip (δ_R = 0 degrees) for both configurations is generally of the opposite sign than that typical of a zero reverse thrust (power off) condition.

The side force and rolling moment (Figures 12 and 13) data indicate trends consistent with the yawing moment, with larger C_Y and C_l increments due to rudder for the Refan configuration.

5.1.2 TUFT FLOW VISUALIZATION

A series of tuft runs were made in order to determine visually the extent of reverse thrust impingement on the vertical tail and rudder. Yaw runs were made for the Refan and Basic configurations at a speed of 90 knots (46.4 m/sec) for power off (EPR = 1.0) and for the 59°F detent EPR. The rudder deflection was zero.

Figures 14 and 15 show the baseline power off, Refan-Basic comparison at β = 0 and 15 degrees, respectively. Both configurations show similar flow patterns. At β = 0 degrees the flow is well behaved and attached everywhere. At β = 15 degrees, areas of flow separation and spanwise flow are evident.

Figures 16 and 17 show the tuft patterns for the Refan and Basic configurations with the thrust reversers operating at the 59°F detent EPR for β = 0 and 15 degrees, respectively. Flow separation exists over a large area of the rudder even at β = 0 degrees. However, the separated region on the Basic configuration rudder is noticeably more disturbed and extends over a greater area than that on the Refan rudder.

These observations agree well with the force data results which indicate a higher rudder effectiveness for the Refan airplane.

5.2 EFFECT OF THRUST REVERSER CLOCK ANGLE

Effect of the Refan configuration target thrust reverser clock angle on the degree of "tail blanking" was investigated. Test clock angles and their

definition are shown in Figure 18. The zero degree angle represents the baseline thrust reverser design. Clocking the reversers outboard turns the reverse jet flow away from the vertical tail and is designed to minimize "tail blanking". Inboard clocking would increase "tail blanking". It was tested since it is one means of reducing engine re-ingestion.

Figure 19 gives rudder effectiveness ($C_{N_{\delta R}}$) as a function of airspeed for clock angles of zero degrees, 20 degrees outboard and 20 degrees inboard, with the engines operating at maximum EPR. Data are shown at β = 0 and 15 degrees. Outboard clocking does not have a significant effect. The data are generally similar to the zero clock angle results. However, inboard clocking leads to a major reduction in rudder effectiveness. For β = 0 degrees and speeds greater than 90 knots (46.4 m/sec) rudder effectiveness is zero. Such a configuration is not recommended, since rudder is the primary means of directional control at the high speed end of the landing rollout.

Airplane yawing moment at β = 15 degrees is given in Figure 20 for the three clock angles as a function of airspeed. The data are at maximum EPR and for δ_R = 0 degrees. The yawing moments are small and there are no major differences between clock angles.

5.3 EFFECT OF THRUST REVERSER LIP AND FENCE CONFIGURATION

A series of Refan target thrust reverser lip and fence configurations were tested in order to determine their effect on "tail blanking". Lips and fences are used to improve thrust reverser efficiency. Variations in size and shape can be used to tailor the reverse thrust flow direction in order to improve engine re-ingestion characteristics. The configurations tested are defined in Figure 21. Lips are located on the top and bottom of each thrust reverser

door and fences along each side, spanning approximately half the door length.

The 3.5 inch (8.89 cm) constant chord lip, with fences on all doors, represents the baseline configuration. The 3.5 inch (8.89 cm) tapered chord lip, tapers to a one inch (2.54 cm) depth at the outboard edge of each door. In addition, the fences at the outboard edge of each door are removed. This configuration is designed to direct the flow away from the vertical tail. The 1.5 inch (3.81 cm) constant chord lip, with fences on all doors, is designed to minimize engine re-ingestion by reducing the degree of T/R flow reversal.

Rudder effectiveness for the three lip/fence configurations is shown as a function of airspeed in Figure 22. The data are for maximum EPR with the Refan reversers at zero clock angle. Variations in lip/fence geometry have very little effect on $C_{N_{\delta R}}$ for speeds down to 90 knots (46.4 m/sec). At lower speeds the baseline 3.5 inch (8.89 cm) constant chord lip is slightly better than the other two configurations.

Lip/fence configuration has only a minor effect on airplane yawing moment due to sideslip. Data at β = 15 degrees and maximum EPR (Figure 23) indicate very little variation between the three configurations.

5.4 ASYMMETRIC REVERSE THRUST CHARACTERISTICS

One engine out reverse thrust runs were made with the Refan target reverser at a maximum EPR power setting. Left and right engines out were tested with zero and full left rudder. Figure 24 presents rudder effectiveness data at β = 0 and 15 degrees as a function of airspeed. Power off (EPR = 1.0) and both engines on, as well as left and right engine out data are shown.

No unusual asymmetric reverse thrust characteristics were noted. The reduction in rudder effectiveness due to each engine operating individually adds up to approximately the $C_{N_{\delta R}}$ level with both engines operating.

5.5 EFFECT OF GROUND PLANE VELOCITY

The moving belt ground plane was utilized throughout the major portion of the test to improve the simulation of ground effect. Near the end of the test, mechanical difficulties with the belt necessitated completion of the test without ground plane motion. Basically, only the engine-out portion of the test was affected.

An example of the effect of ground plane motion on yawing moment and side force data is shown in Figure 25. The data are plotted versus sideslip angle with the right engine inoperative and the left one at maximum EPR. For an airspeed of 90 knots (46.4 m/sec), the effect between a stationary ground plane and one moving at 90 knots (46.4 m/sec) is shown. The effect on yawing moment and side force, although noticeable, is not considered of sufficient magnitude to invalidate the engine out test results.

5.6 DATA REPEATABILITY

Runs were made throughout the test to check data repeatability. An example is shown in Figure 26. C_N, C_Y and C_l are plotted versus sideslip angle for the Refan configuration at maximum EPR and an airspeed of 110 knots (56.6 m/sec). Data repeatability is excellent for side force and rolling moment, and is considered adequate for yawing moment.

6.0 CONCLUSIONS

The effects of installing the P&W Refan JT8D-100 series engine with its target thrust reverser on the Boeing 727-200 airplane, were investigated in a low-speed wind tunnel test. Directional control characteristics, with the thrust reversers operating, were evaluated with the airplane in the landing configuration in ground effect and under crosswind conditions. A direct comparison was made with the Basic 727-200 with its clamshell-deflector door thrust reverser configuration.

Refan airplane directional control characteristics, with thrust reversers operating, are slightly improved relative to those of the Basic 727 airplane. Therefore, thrust reverser clocking, in order to reduce the "tail blanking" effect, is not considered necessary.

Clocking the Refan target reversers 20 degrees outboard, to direct the flow away from the vertical tail, has only a minor effect on directional control. However, clocking the reversers 20 degrees inboard, results in a virtual loss of rudder control at maximum EPR for speeds above 90 knots (46.4 m/sec), especially at small sideslip angles. The latter configuration is not considered acceptable, since the rudder is the primary means of directional control during the high speed segment of the landing rollout.

The Refan thrust reverser lip and fence configurations tested have only a minor effect on airplane directional control characteristics.

Asymmetric operation of the Refan thrust reversers does not produce any unusual directional control characteristics.

7.0 LIST OF FIGURES

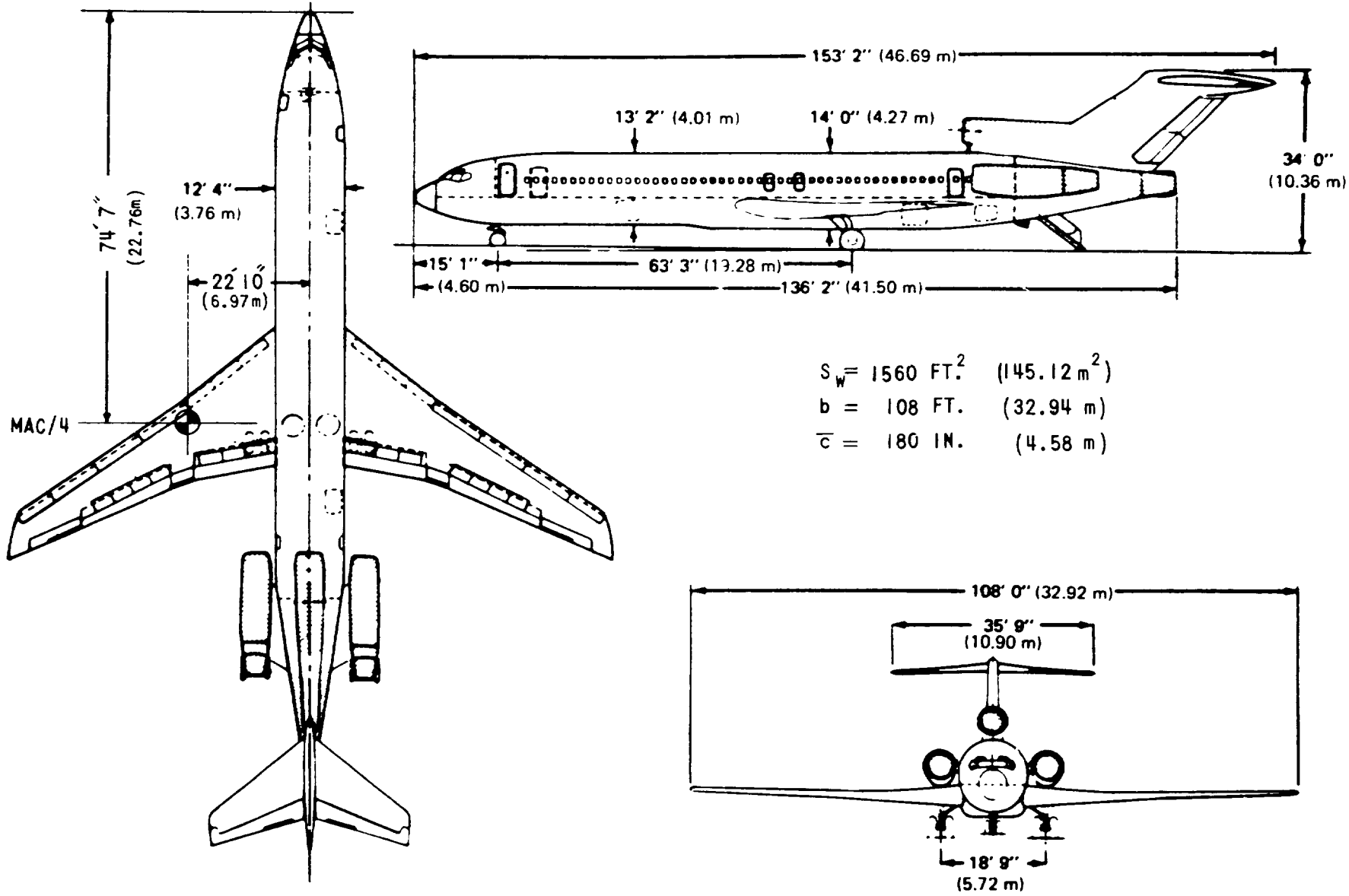

FIGURE 1.- 727-200 REFAN AIRPLANE

FIGURE 2.- 727-200 REFAN MODEL INSTALLED IN THE BOEING-VERTOL LOW-SPEED WIND TUNNEL

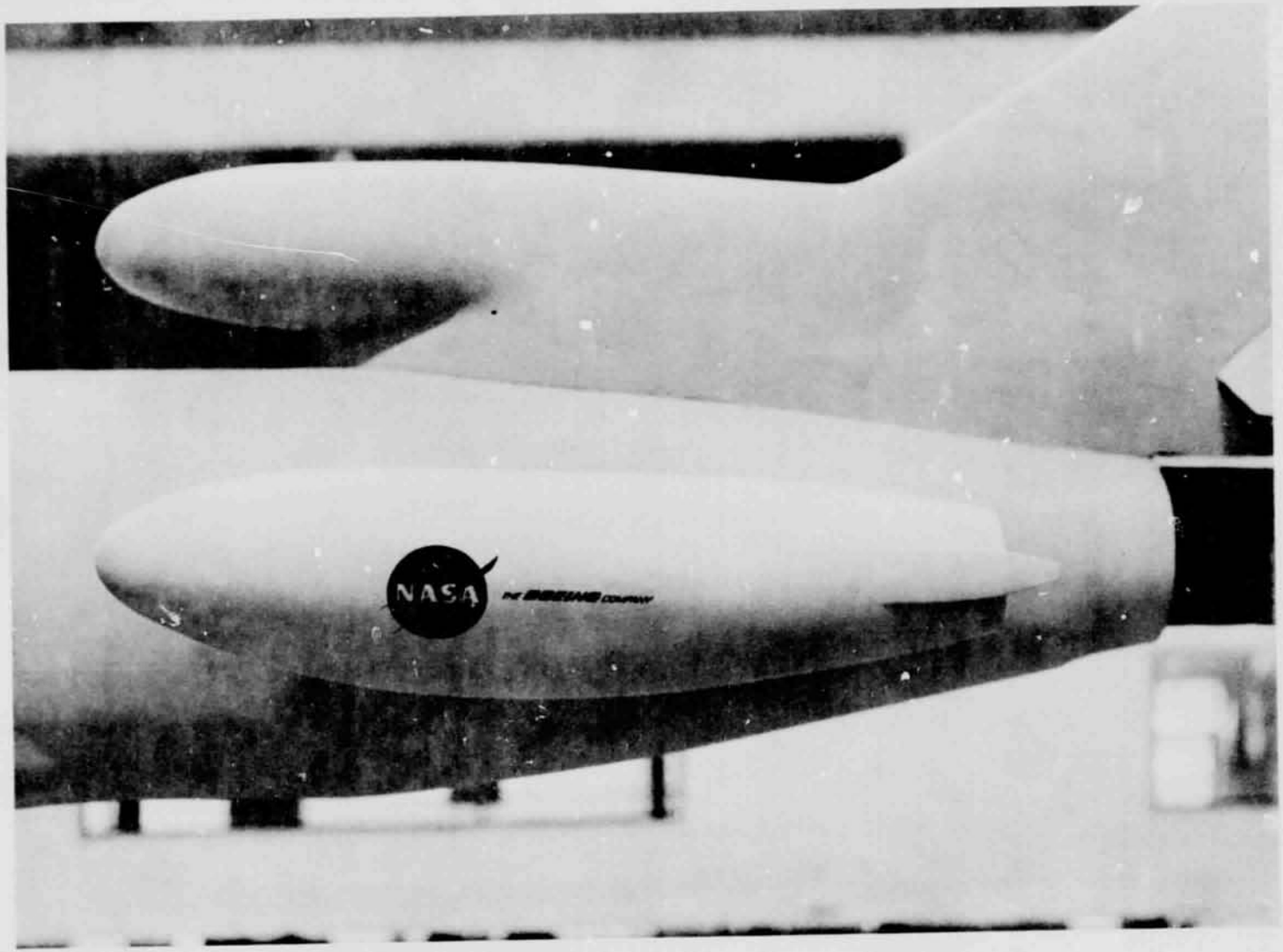

FIGURE 3.- 727-200 REFAN BLOWING SIDE NACELLE INSTALLATION. T/R STOWED.

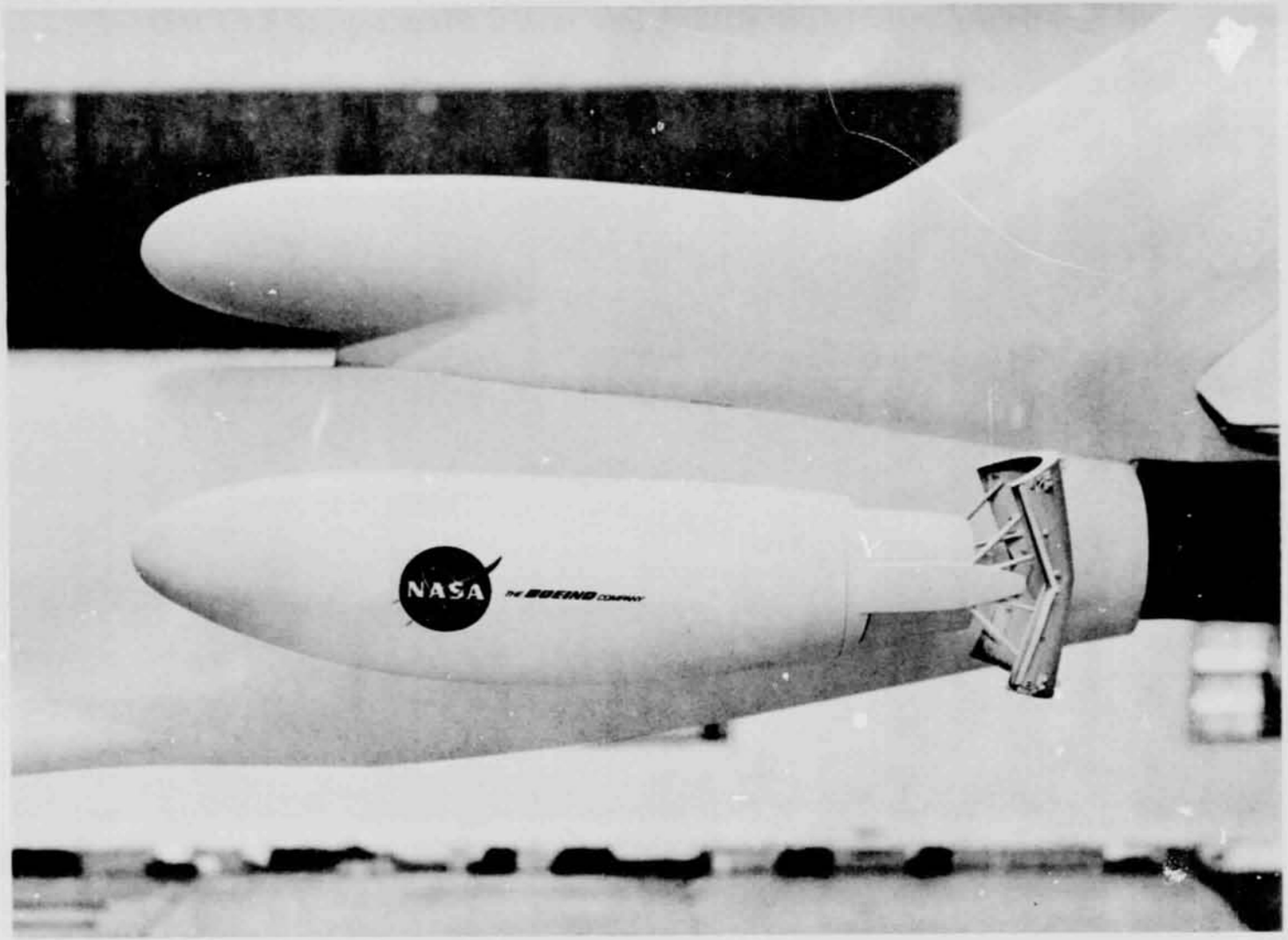

FIGURE 4.- 727-200 REFAN BLOWING SIDE NACELLE INSTALLATION. T/R DEPLOYED

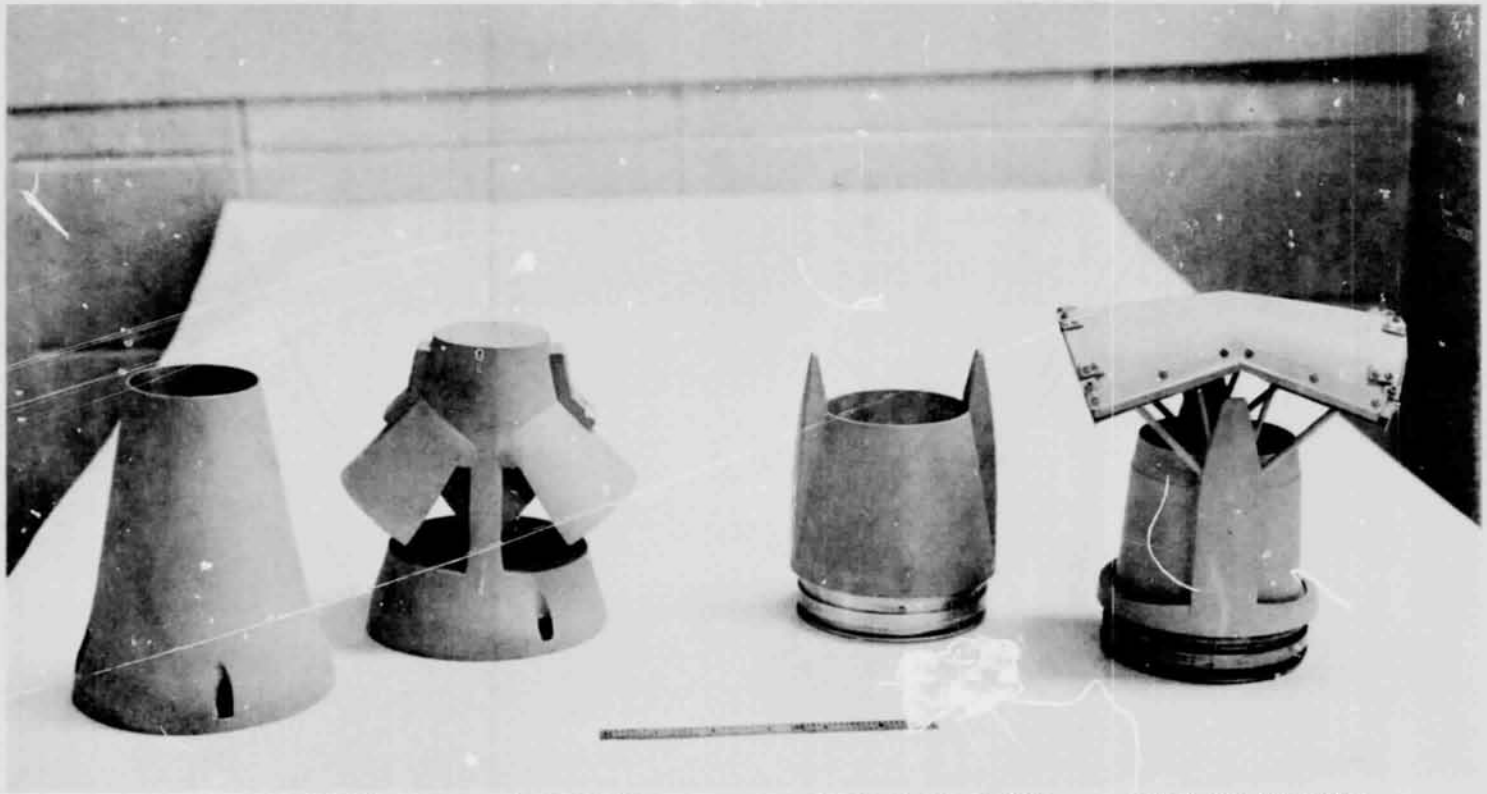

BASIC CLEAN NOZZLE BASIC T/R DEPLOYED (CLAMSHELL-DEFLECTOR DOOR) REFAN CLEAN NOZZLE REFAN T/R DEPLOYED (TARGET)

FIGURE 5.- MODEL TEST NOZZLE AND THRUST REVERSER PARTS

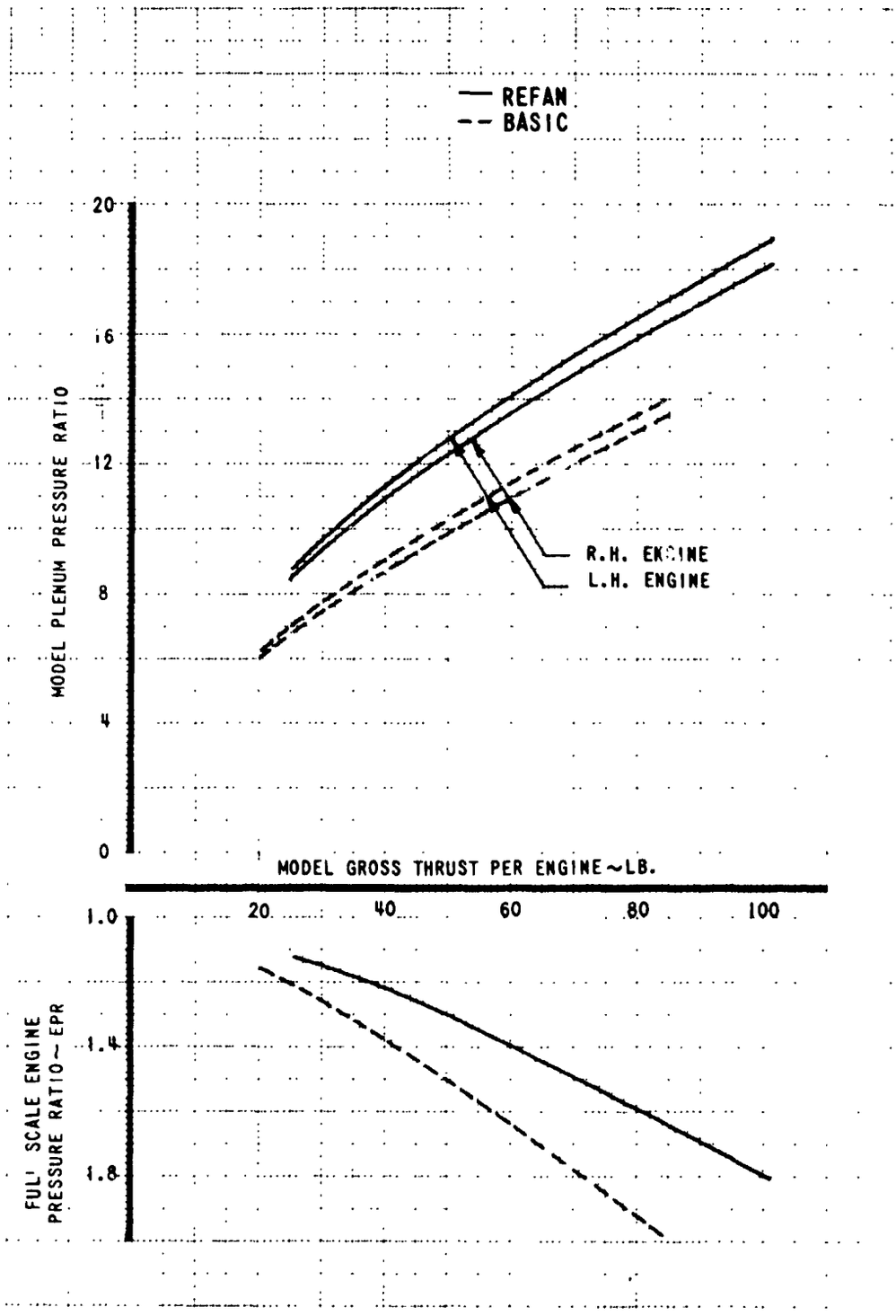

FIGURE 6.- MODEL ENGINE THRUST CALIBRATION, CLEAN NOZZLE

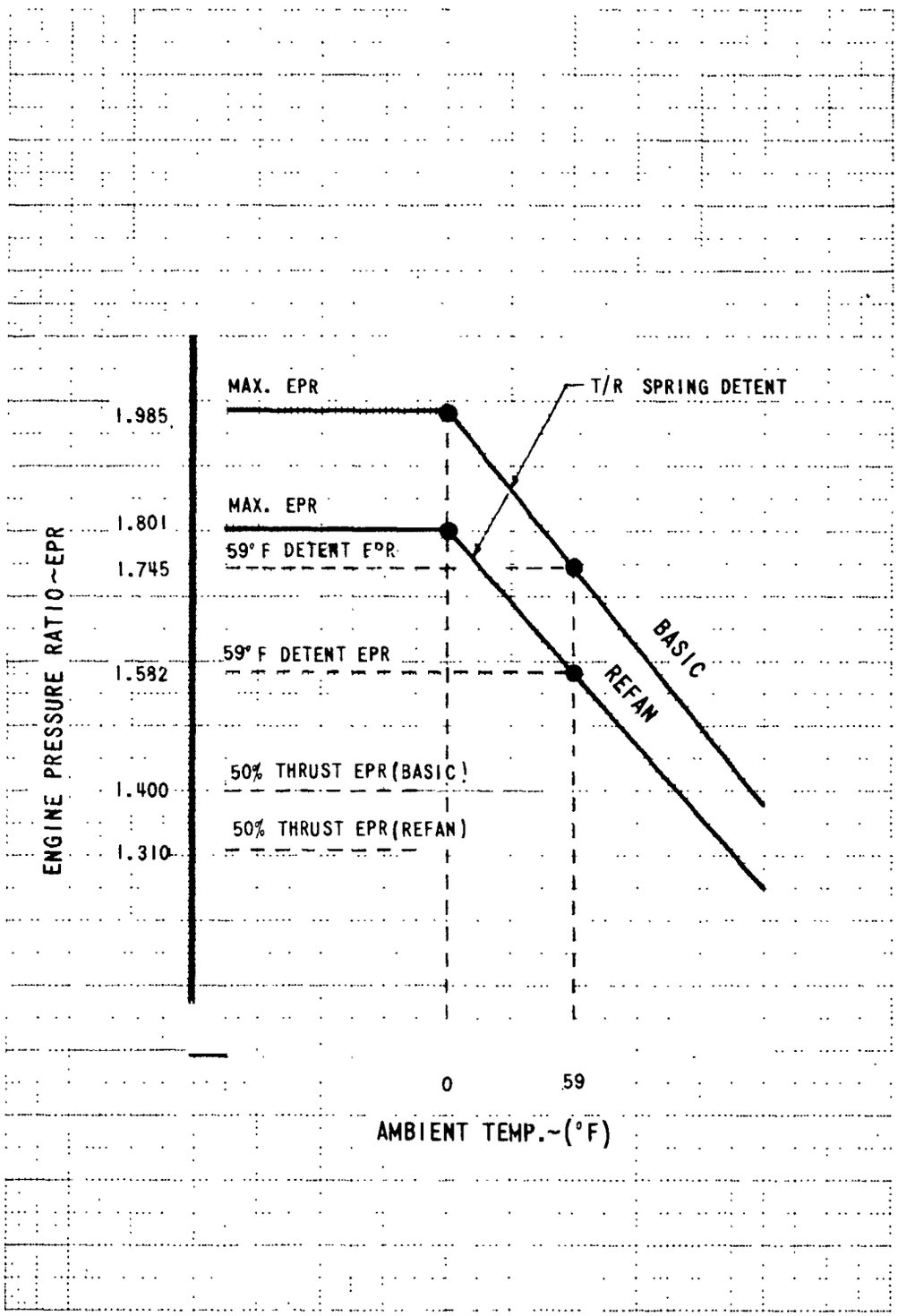

FIGURE 7.- FULL SCALE ENGINE PRESSURE RATIO(EPR) SETTINGS

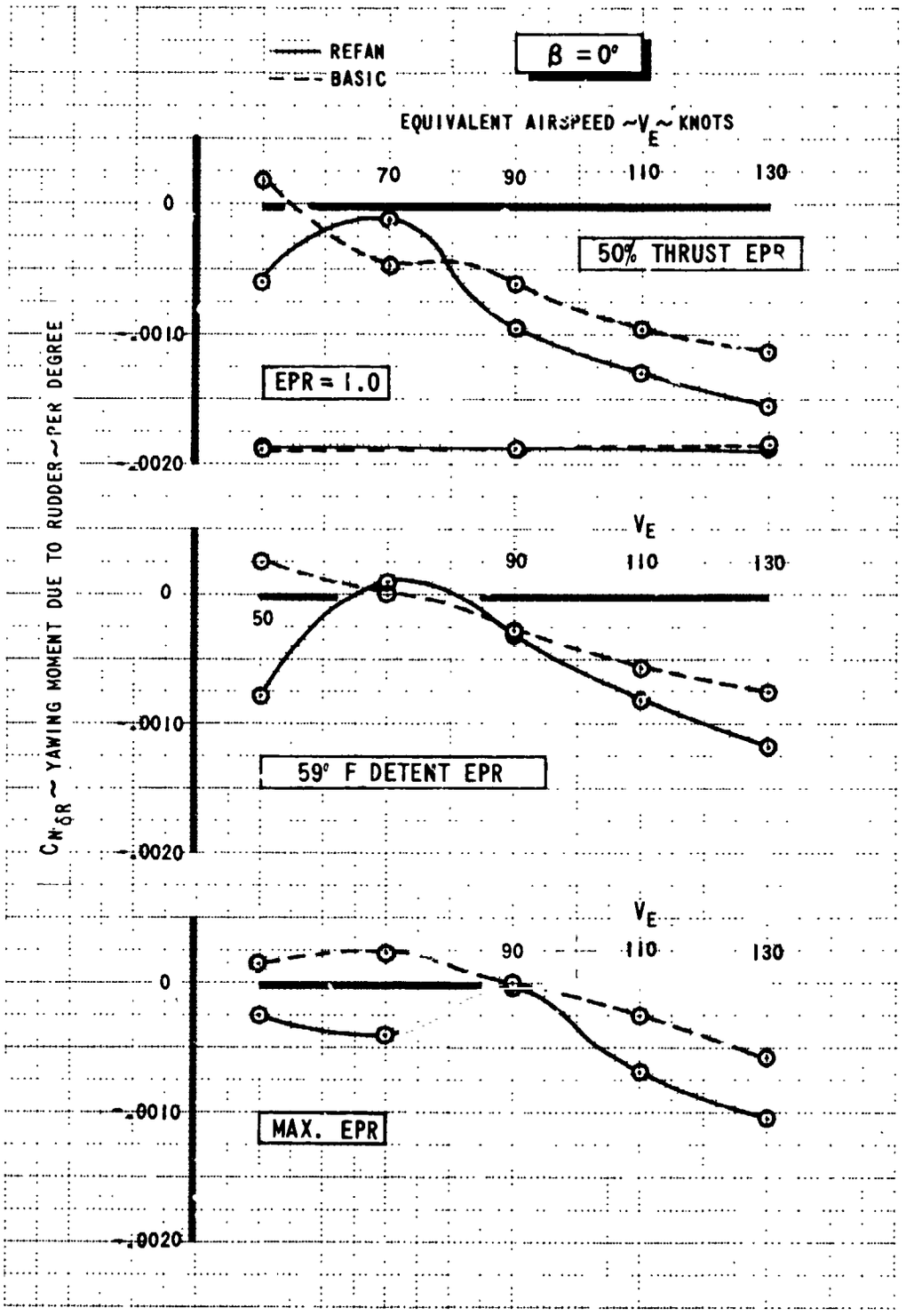

FIGURE 8.- REFAN-BASIC AIRPLANE COMPARISON, RUDDER EFFECTIVENESS, β= 0 DEG.

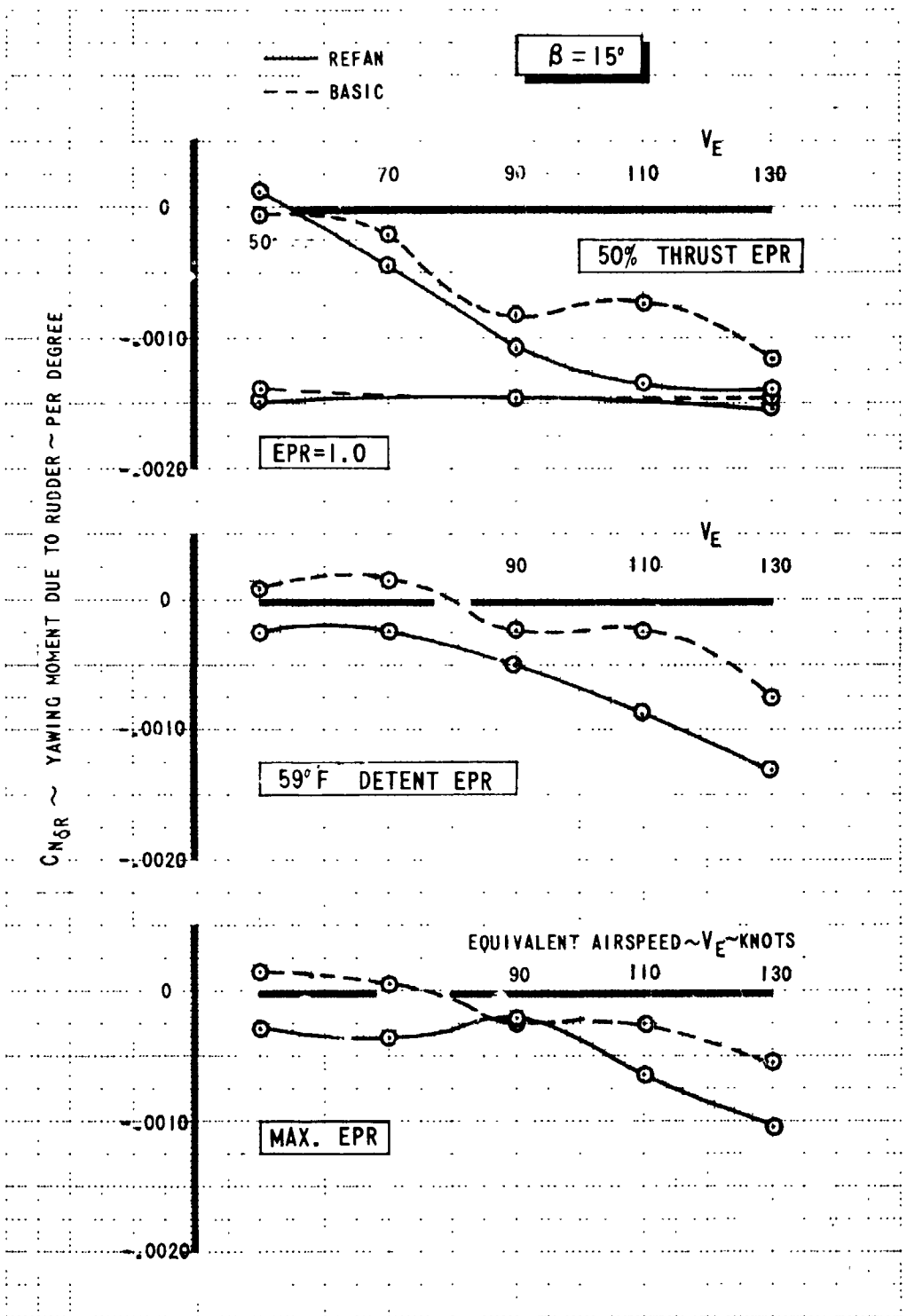

FIGURE 9.- REFAN-BASIC AIRPLANE COMPARISON, RUDDER EFFECTIVENESS, β=15 DEG.

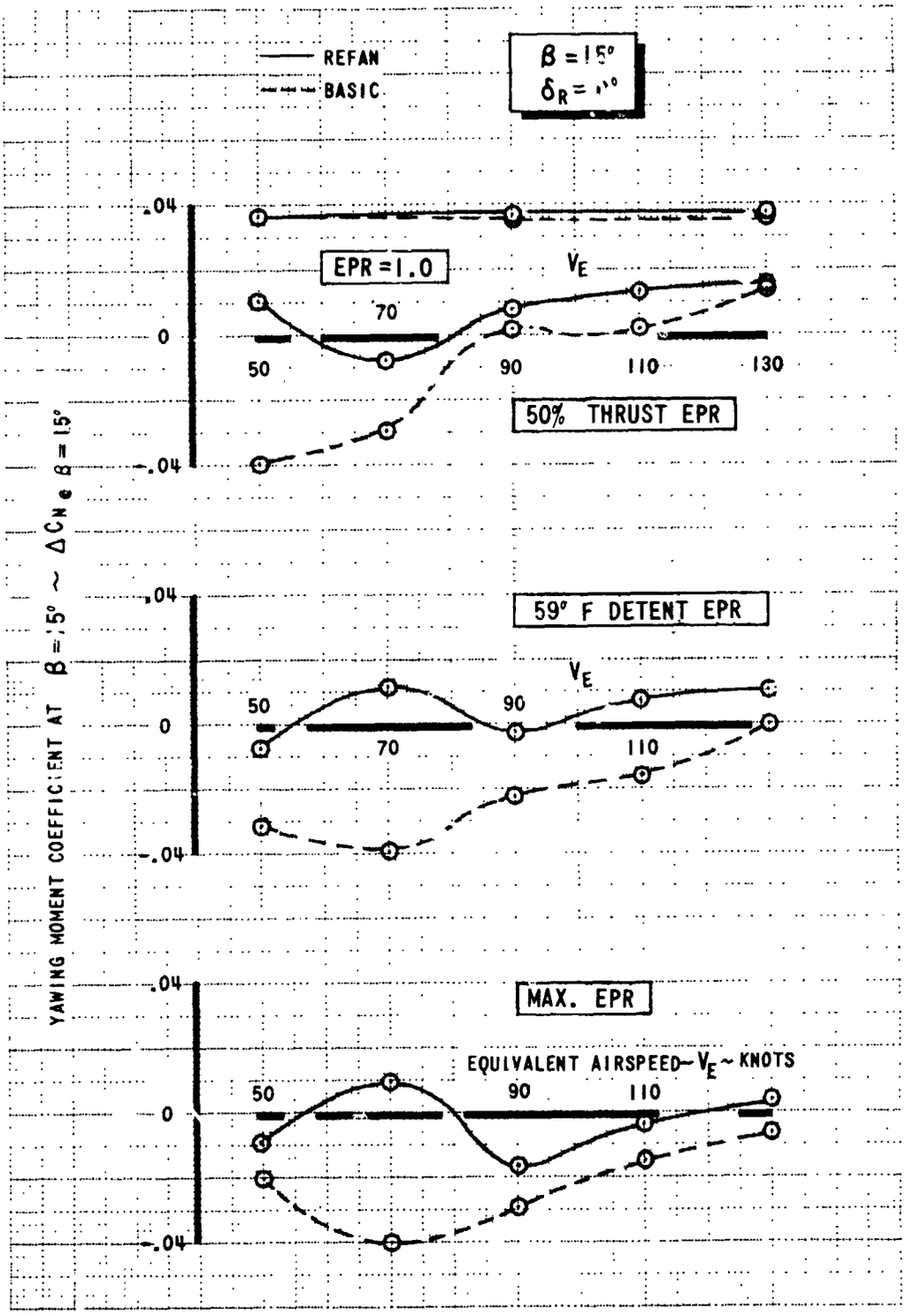

FIGURE 10.- REFAN-BASIC AIRPLANE COMPARISON, YAWING MOMENT DUE TO SIDESLIP, β=15 DEG., δ_R=0 DEG.

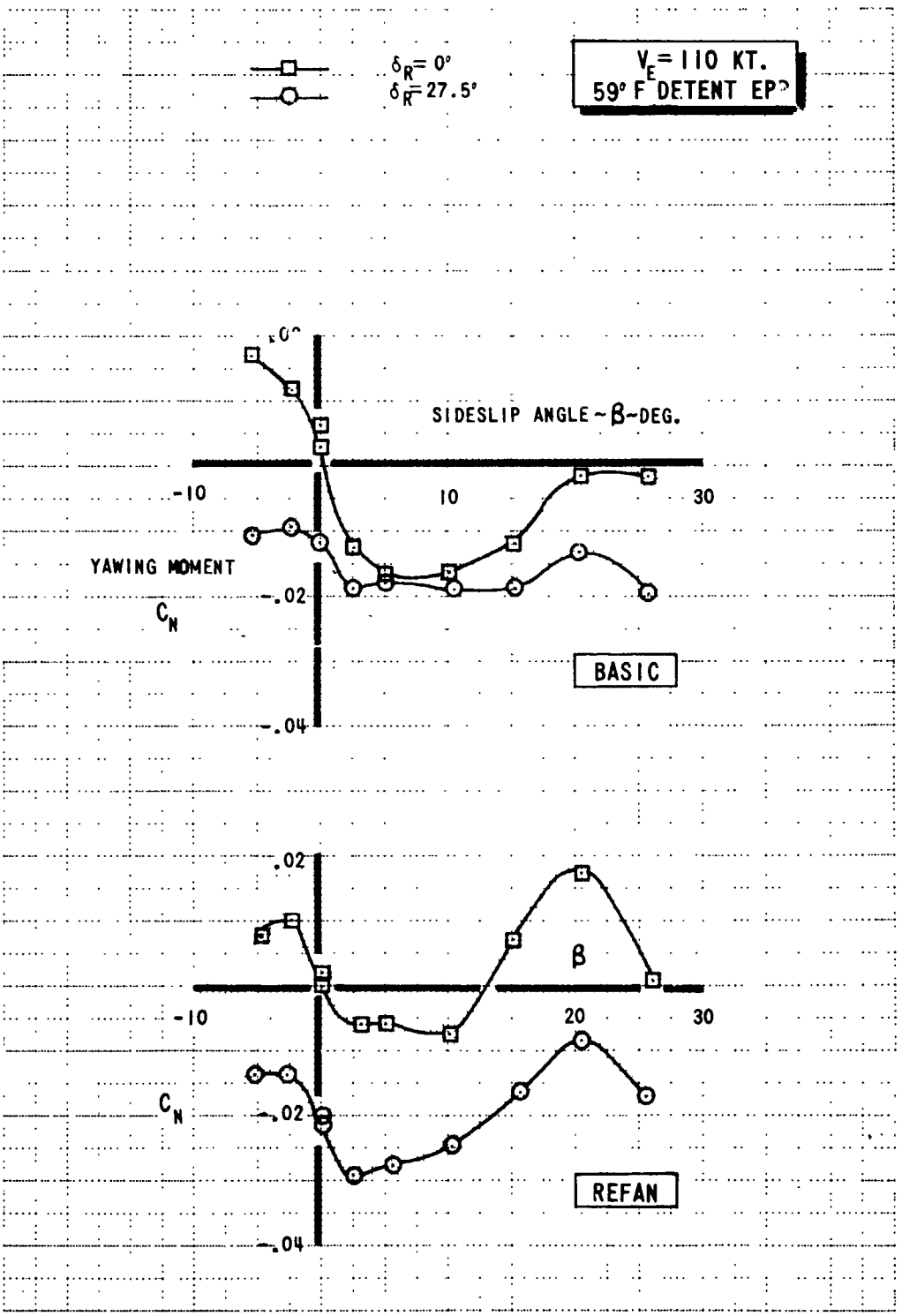

FIGURE 11.- REFAN-BASIC AIRPLANE COMPARISON, C_N vs. β, $V_E = 110$ KT. (56.6 m/sec.), 59° F DETENT EPR

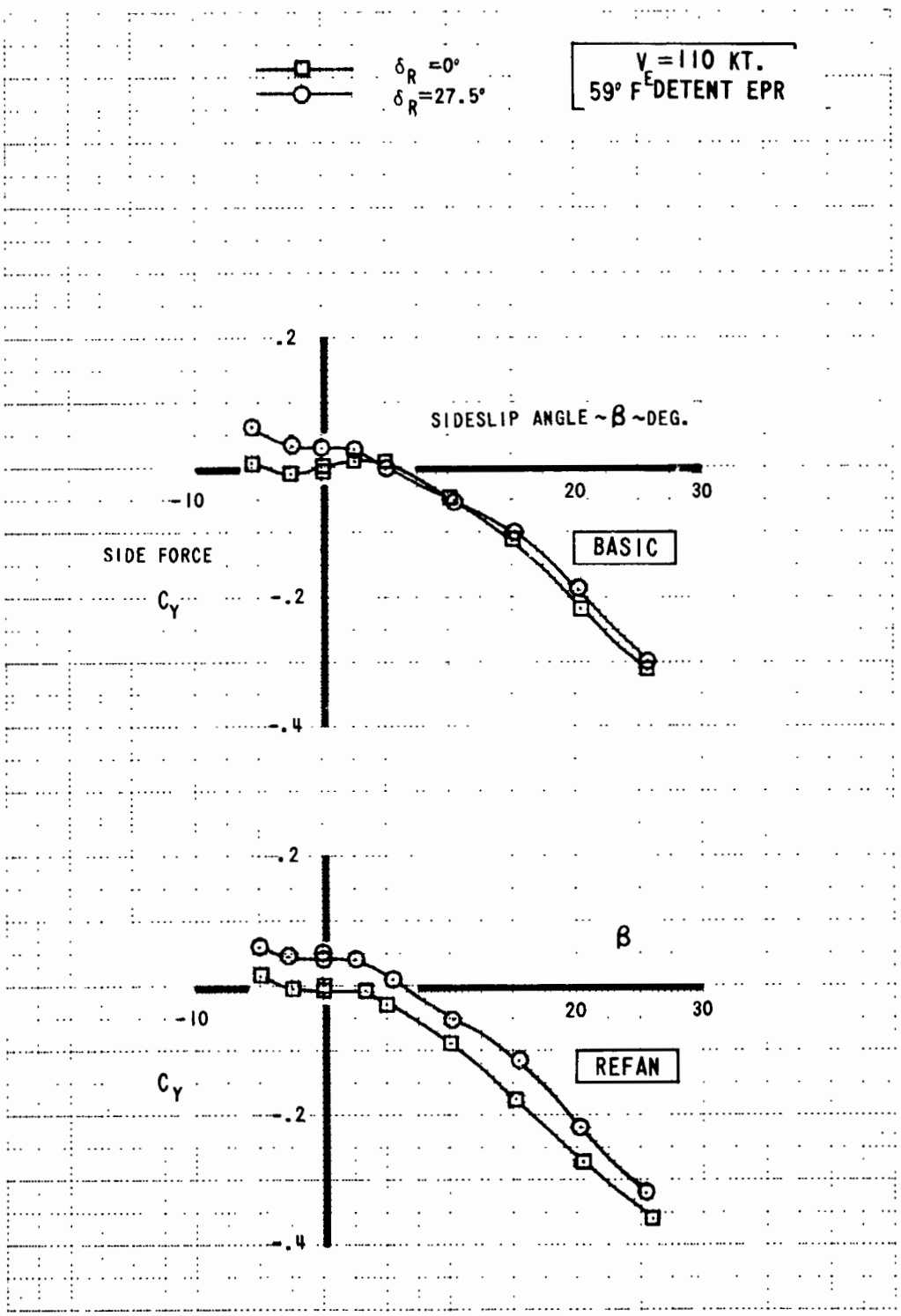

FIGURE 12.- REFAN-BASIC AIRPLANE COMPARISON, C_Y vs. β, V_E=110 KT. (56.6 m/sec.), 59° F DETENT EPR

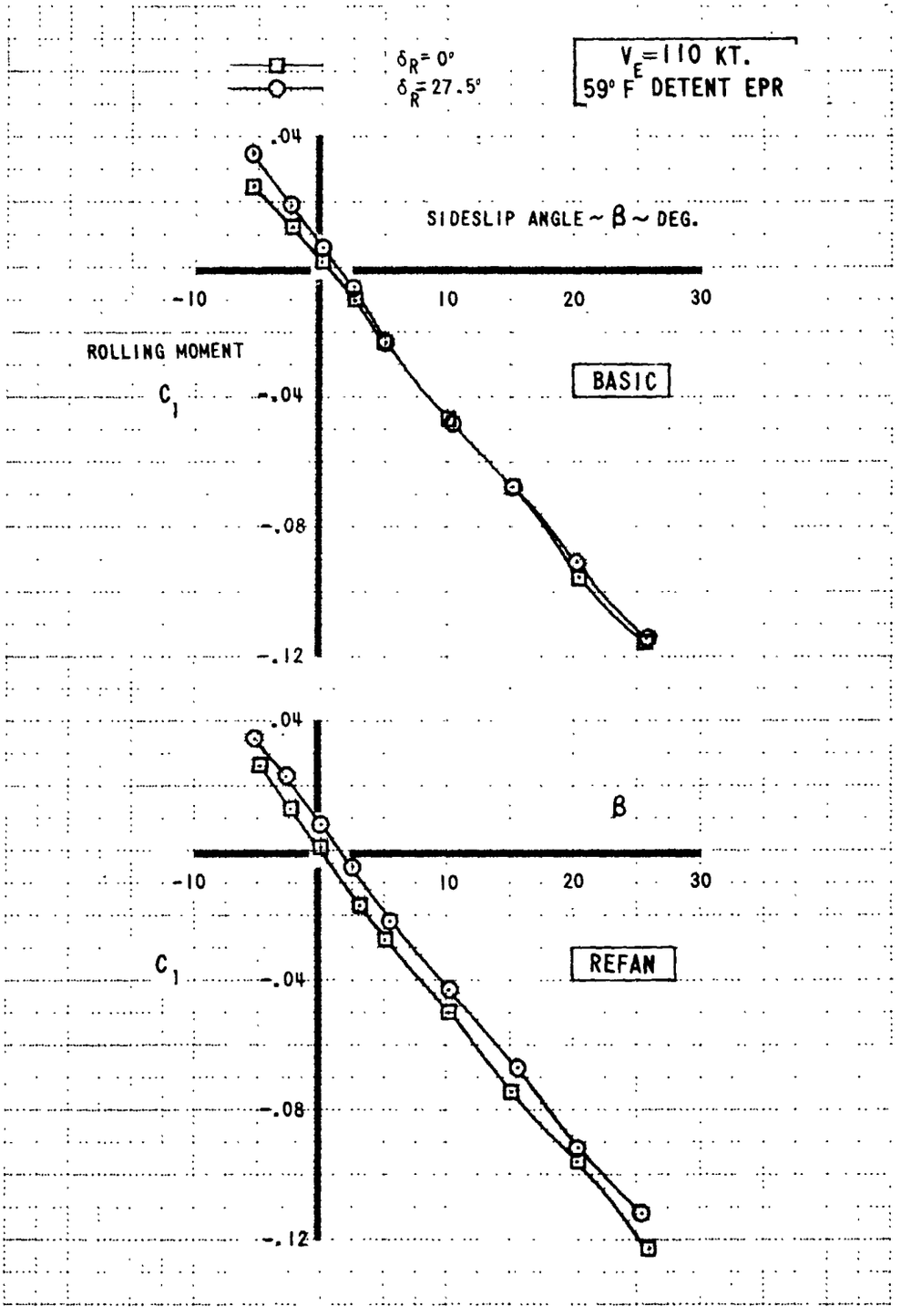

FIGURE 13.- REFAN-BASIC AIRPLANE COMPARISON, C_l vs. β, V_E 110 KT. (56.6 m/sec.), 59° F DETENT EPR

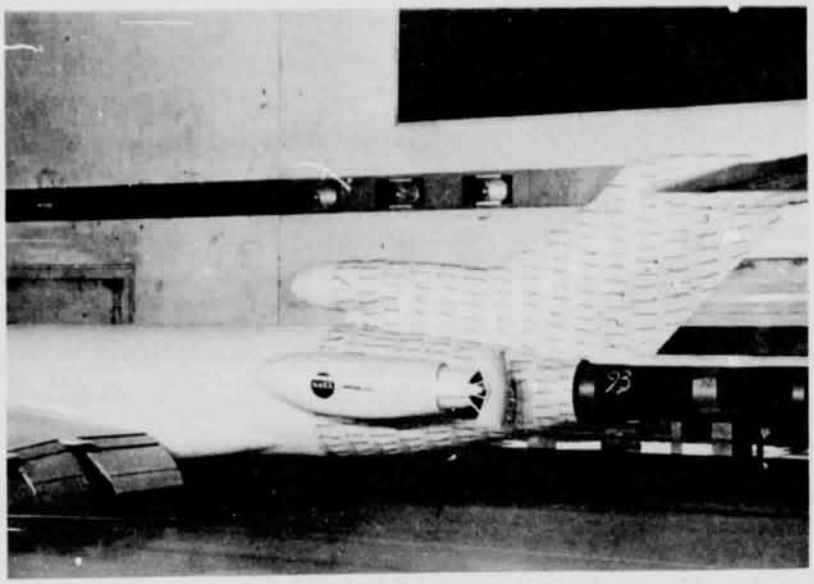

REFAN

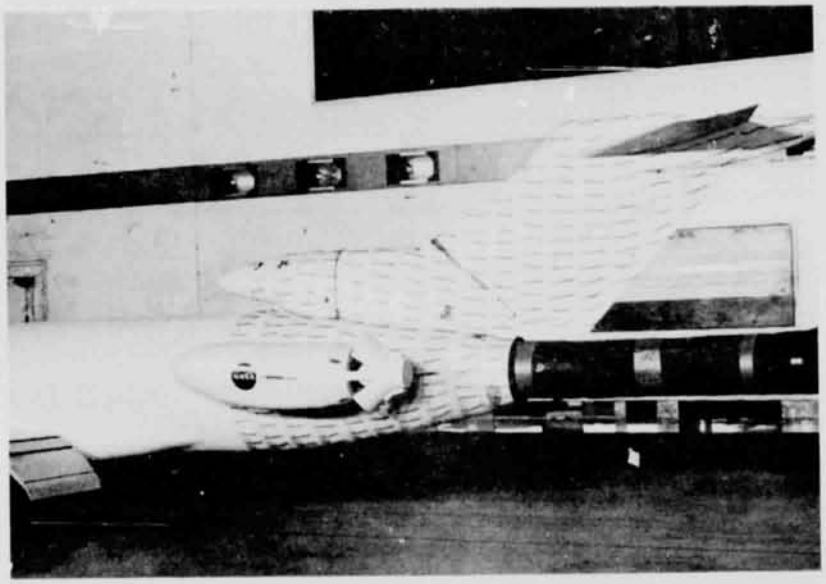

BASIC

FIGURE 14.- TUFT FLOW VISUALIZATION, REFAN-BASIC AIRPLANE COMPARISON, β= 0 DEG., EPR=1.0, V_E=90 KT. (46.4 m/sec.), δ_R= 0 DEG.

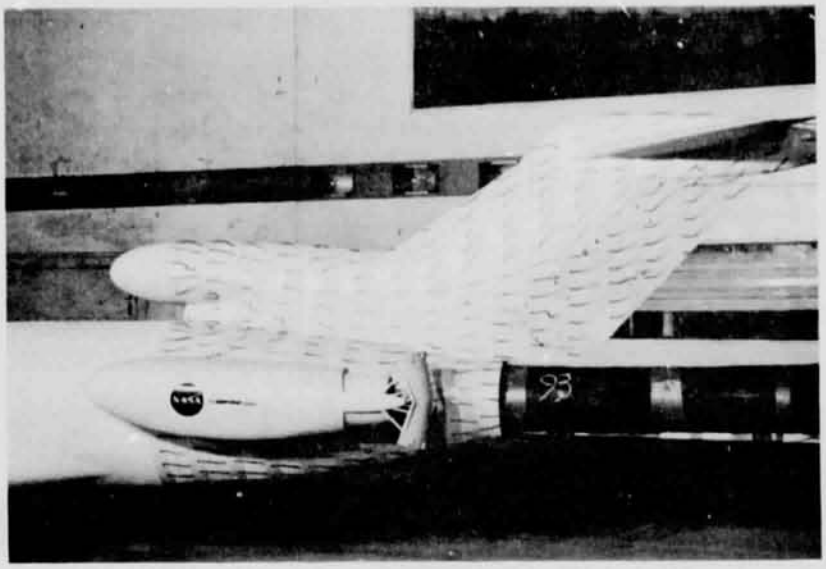

REFAN

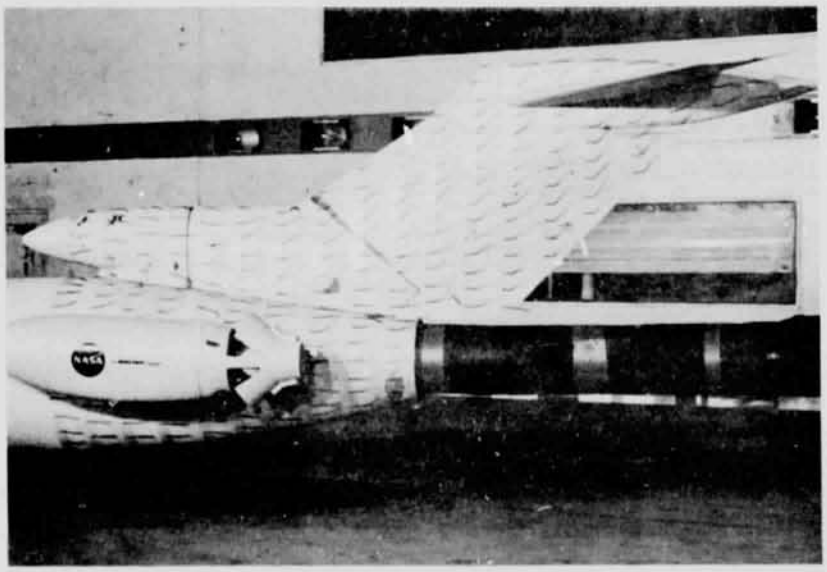

BASIC

FIGURE 15.- TUFT FLOW VISUA' 'ZATION, REFAN-BASIC AIRPLANE COMPARISON, $\beta = 15$ DEG., EPR=1.0, $V_E = 90$ KT.(46.4 m/sec.), $\delta_R = 0$ DEG.

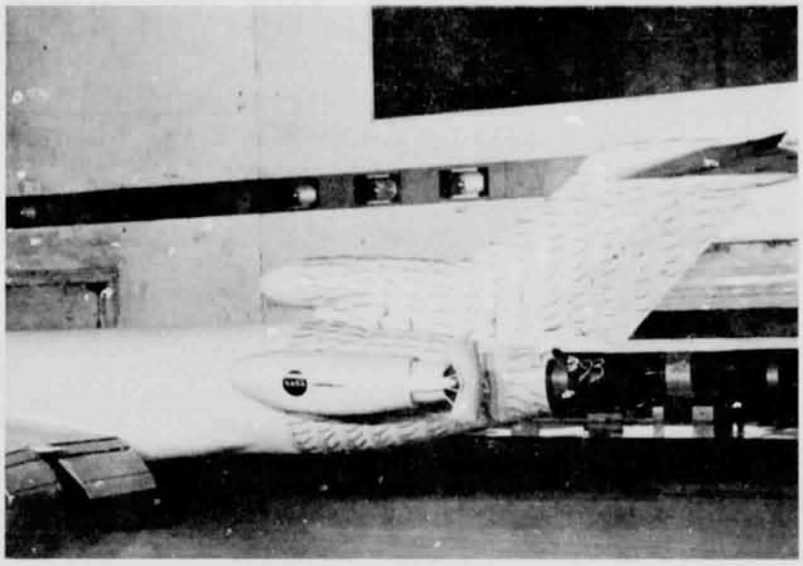

REFAN

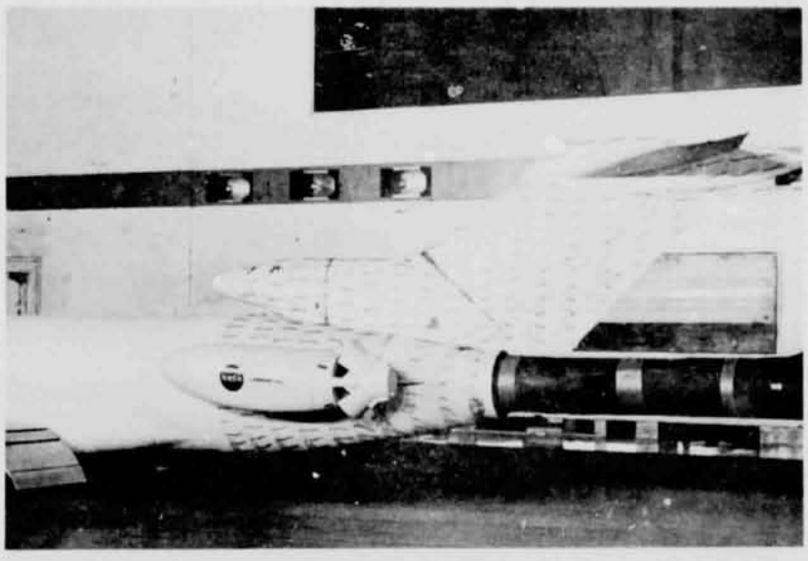

BASIC

FIGURE 16.- TUFT FLOW VISUALIZATION, REFAN-BASIC AIRPLANE COMPARISON, $\beta = 0$ DEG., 59° F DETENT EPR, $V_E = 90$ KT. (46.4 m/sec.), $\delta_R = 0$ DEG.

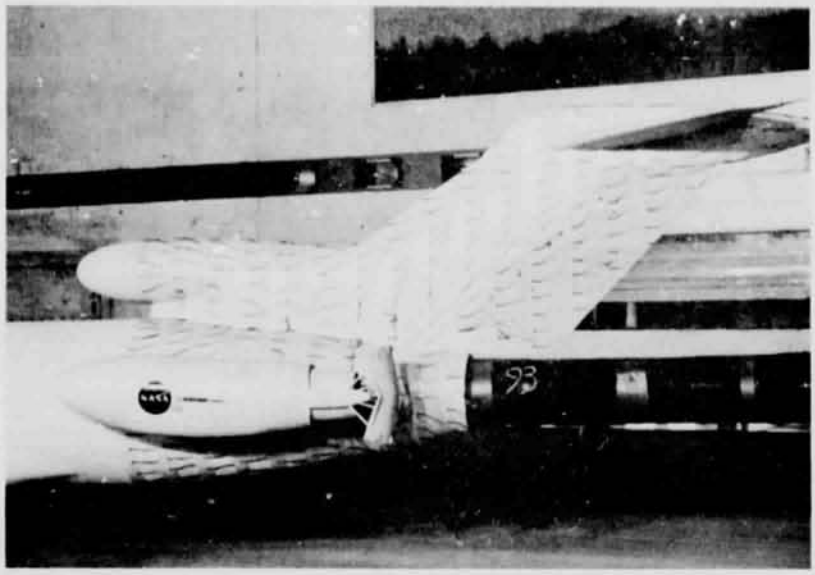

REFAN

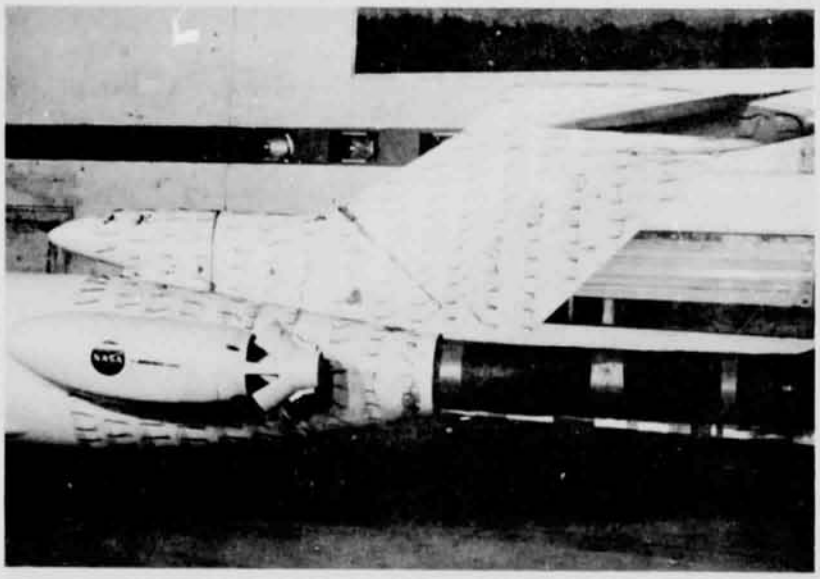

BASIC

FIGURE 17.- TUFT FLOW VISUALIZATION, REFAN-BASIC AIRPLANE COMPARISON, β=15 DEG., 59° F DETENT EPR, V_c=90 KT. (46.4 m/sec.), δ_R= 0 DEG.

727 MODEL, REAR VIEW

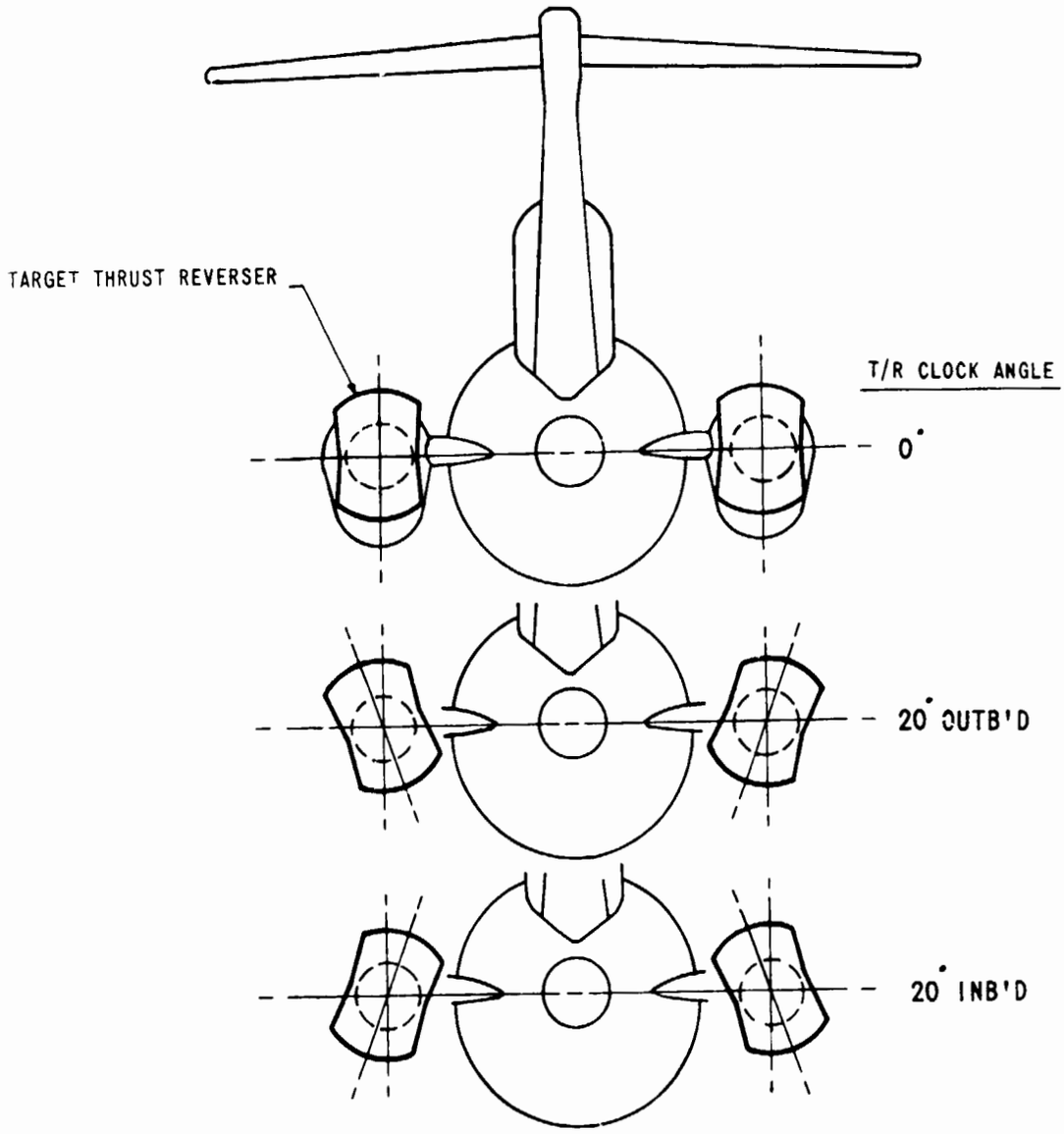

FIGURE 18.- REFAN THRUST REVERSER CLOCK ANGLE DEFINITION

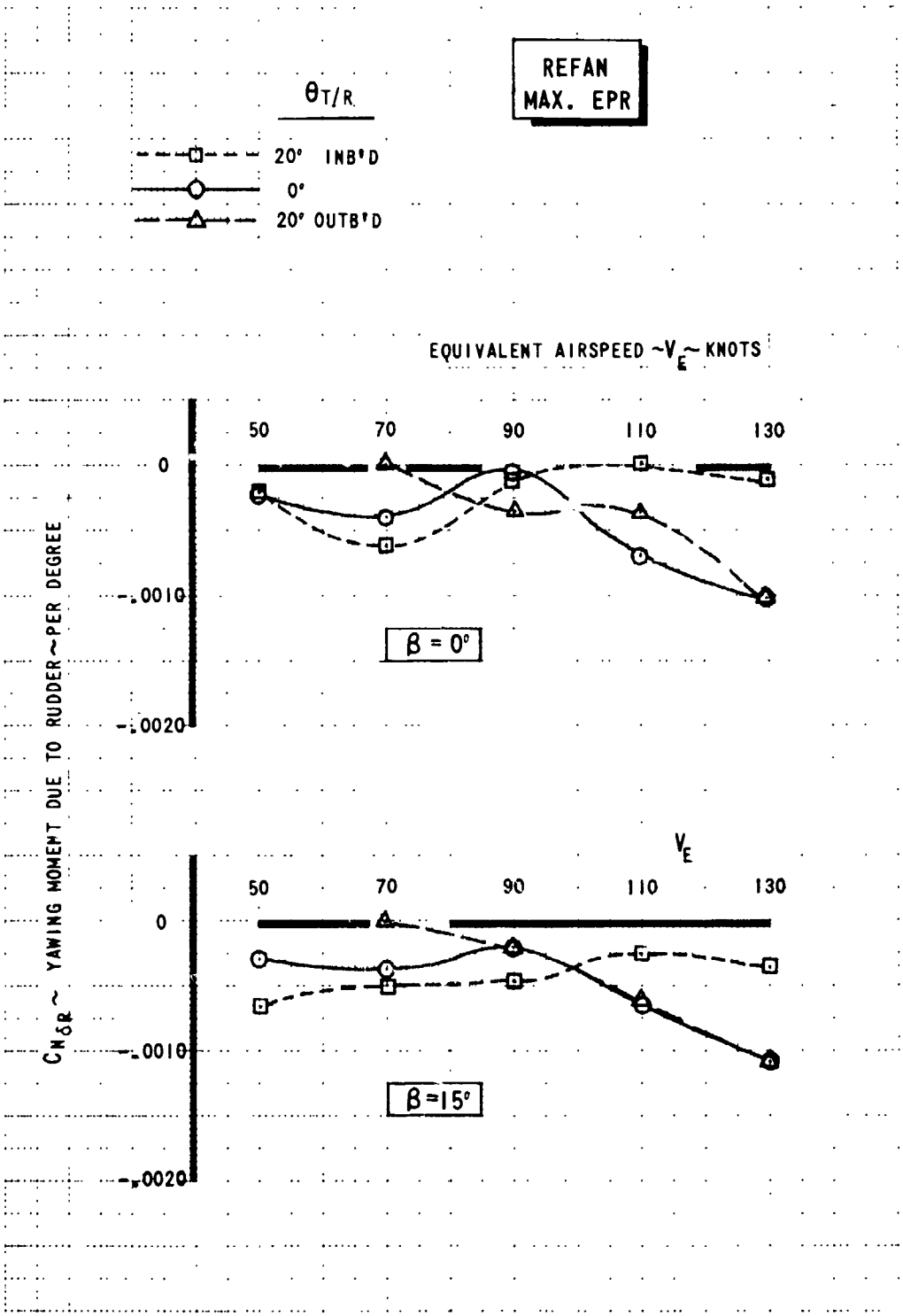

FIGURE 19.- EFFECT OF T/R CLOCK ANGLE, REFAN AIRPLANE, RUDDER EFFECTIVENESS, MAX. EPR

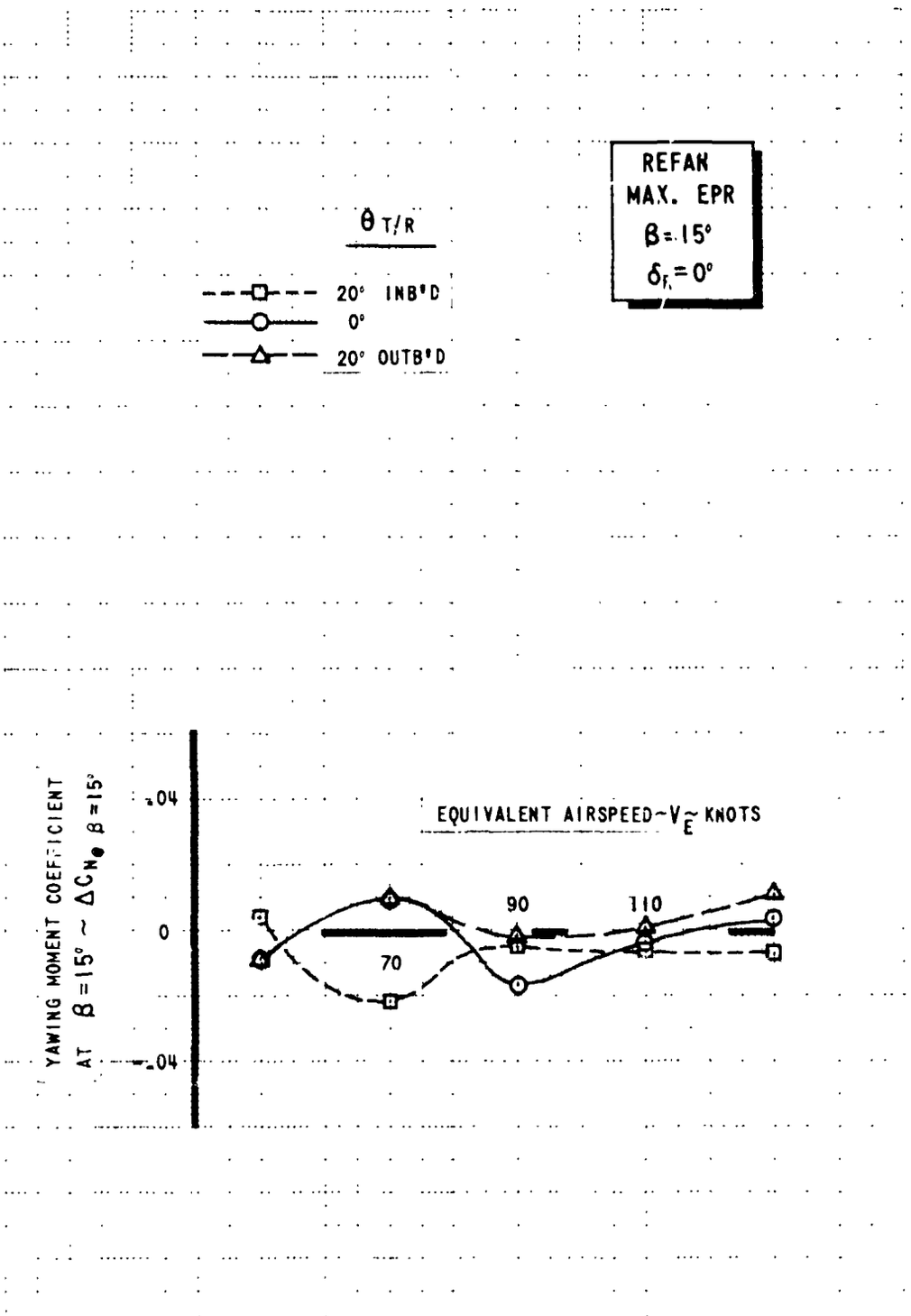

FIGURE 20.- EFFECT OF T/R CLOCK ANGLE, REFAN AIRPLANE, YAWING MOMENT DUE TO SIDESLIP, MAX. EPR, β=15 DEG., δ_R= 0 DEG.

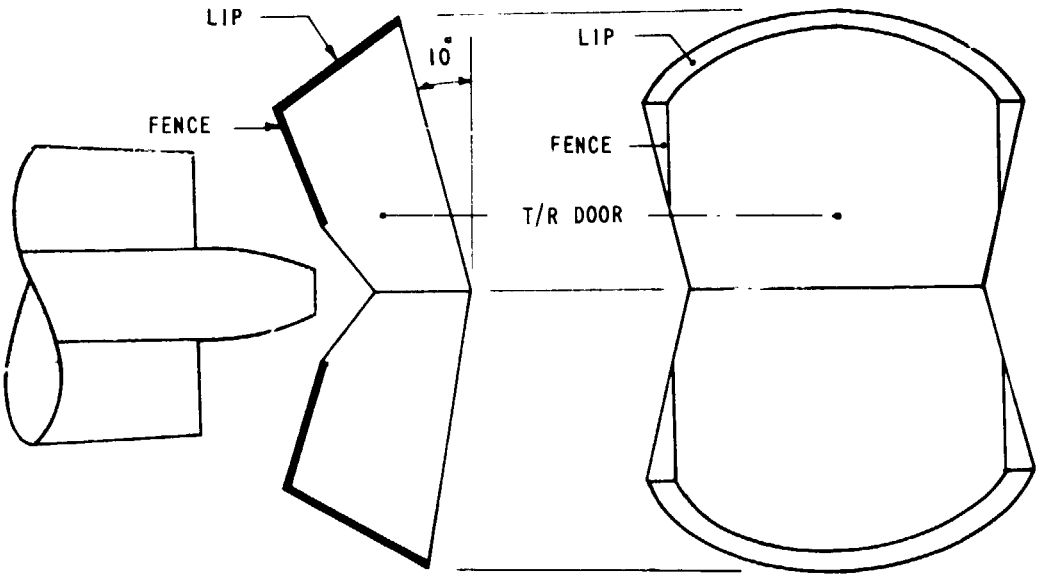

TEST LIP CONFIGURATIONS

3.5 IN. CONSTANT CHORD LIP
(ALL FENCES ON)

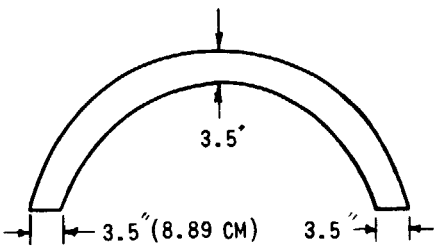

3.5 IN. TAPERED CHORD LIP
(OUTBOARD FENCES ON TOP
AND BOTTOM DOORS REMOVED)

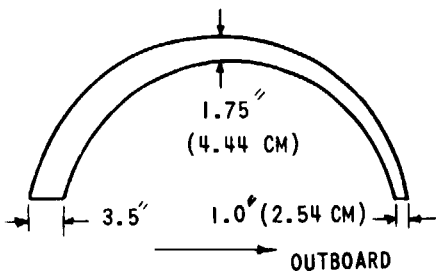

1.5 IN. CONSTANT CHORD LIP
(ALL FENCES ON)

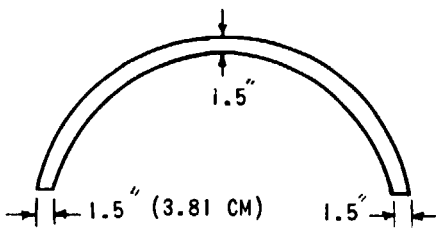

FIGURE 21.- REFAN THRUST REVERSER LIP AND FENCE CONFIGURATIONS

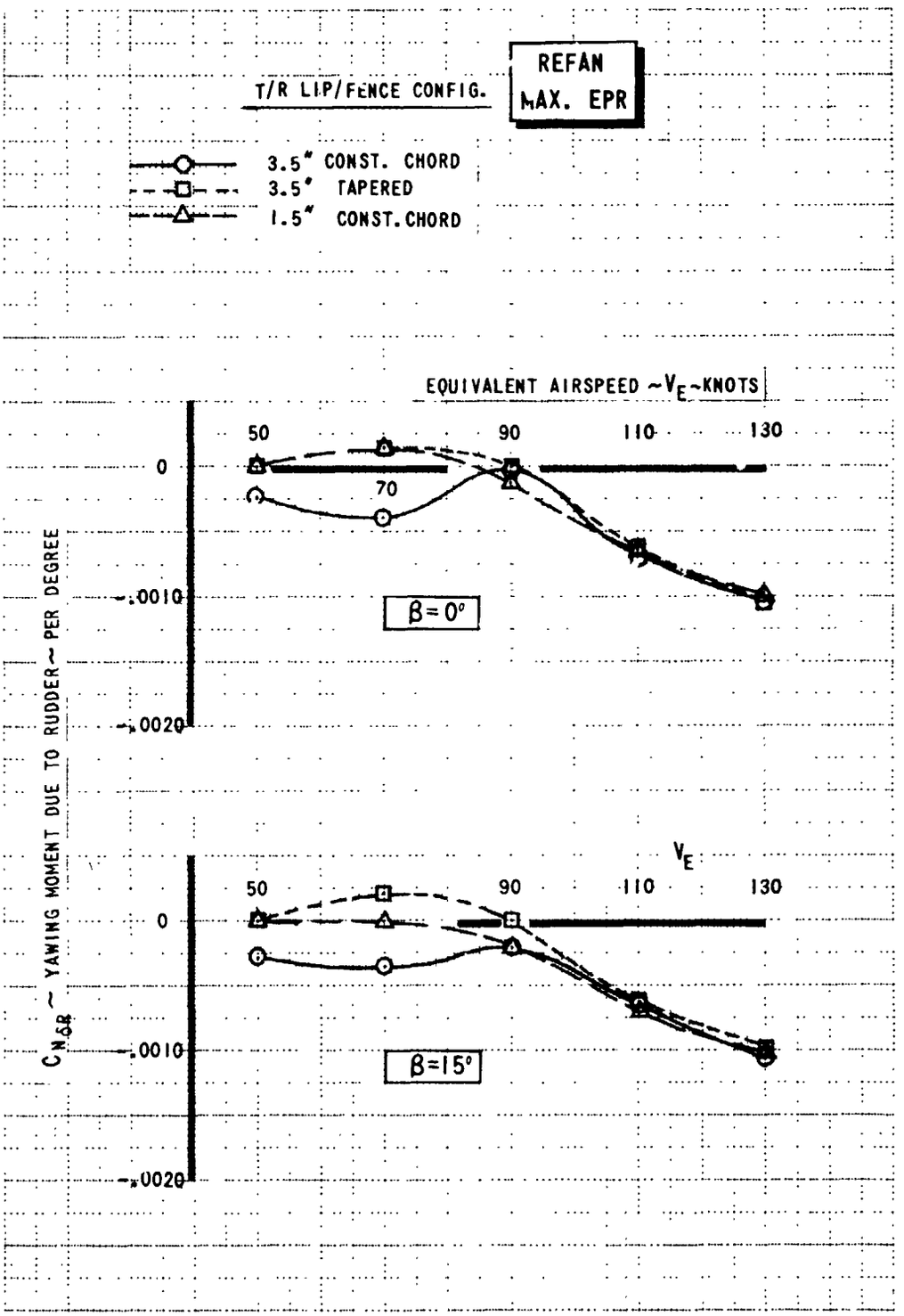

FIGURE 22.- EFFECT OF T/R LIP/FENCE CONFIGURATION, REFAN AIRPLANE, RUDDER EFFECTIVENESS, MAX.EPR,

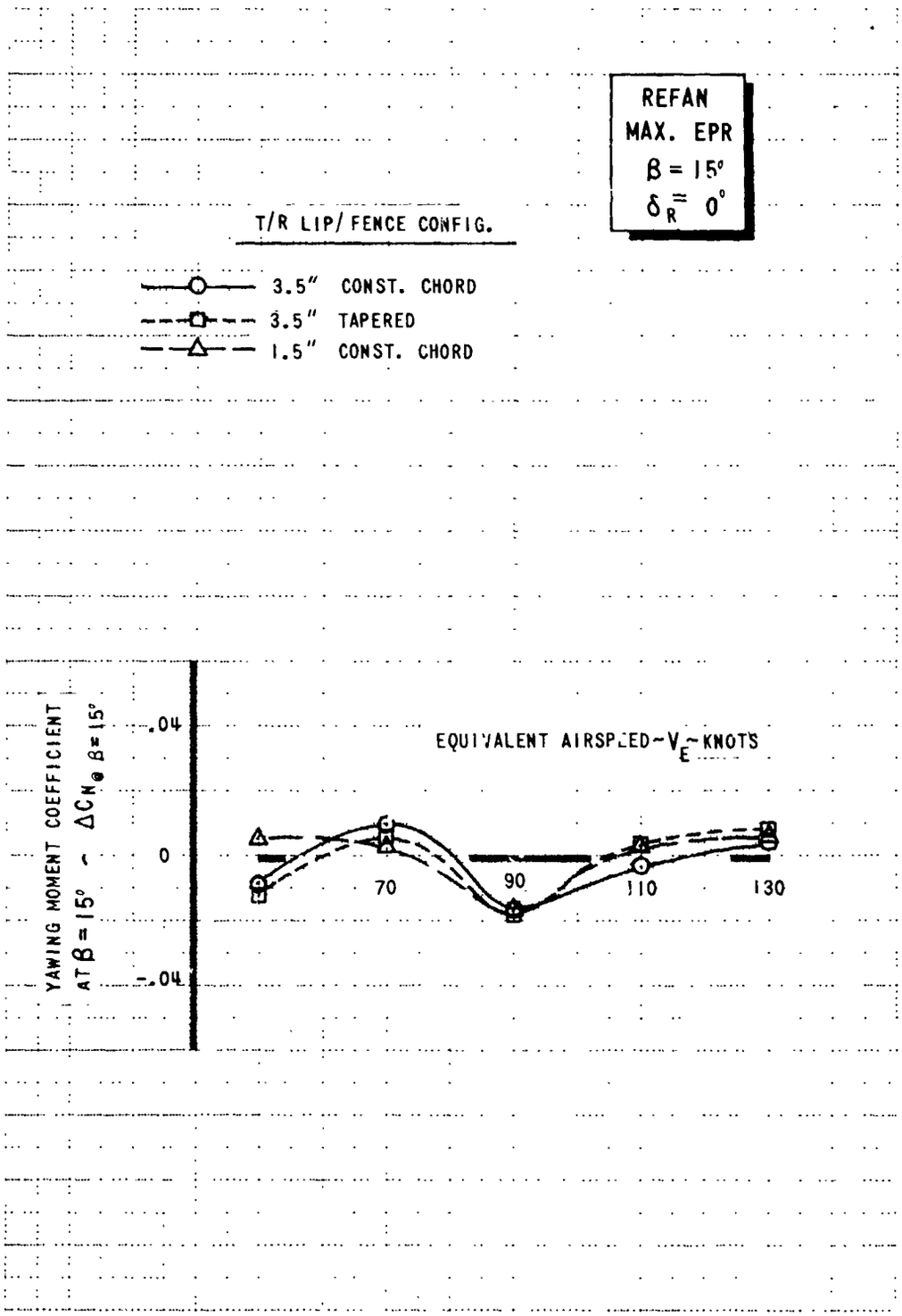

FIGURE 23.- EFFECT OF T/R LIP/FENCE CONFIGURATION, REFAN AIRPLANE, YAWING MOMENT DUE TO SIDESLIP, MAX. EPR , β= 15 DEG., δ_R= 0 DEG.

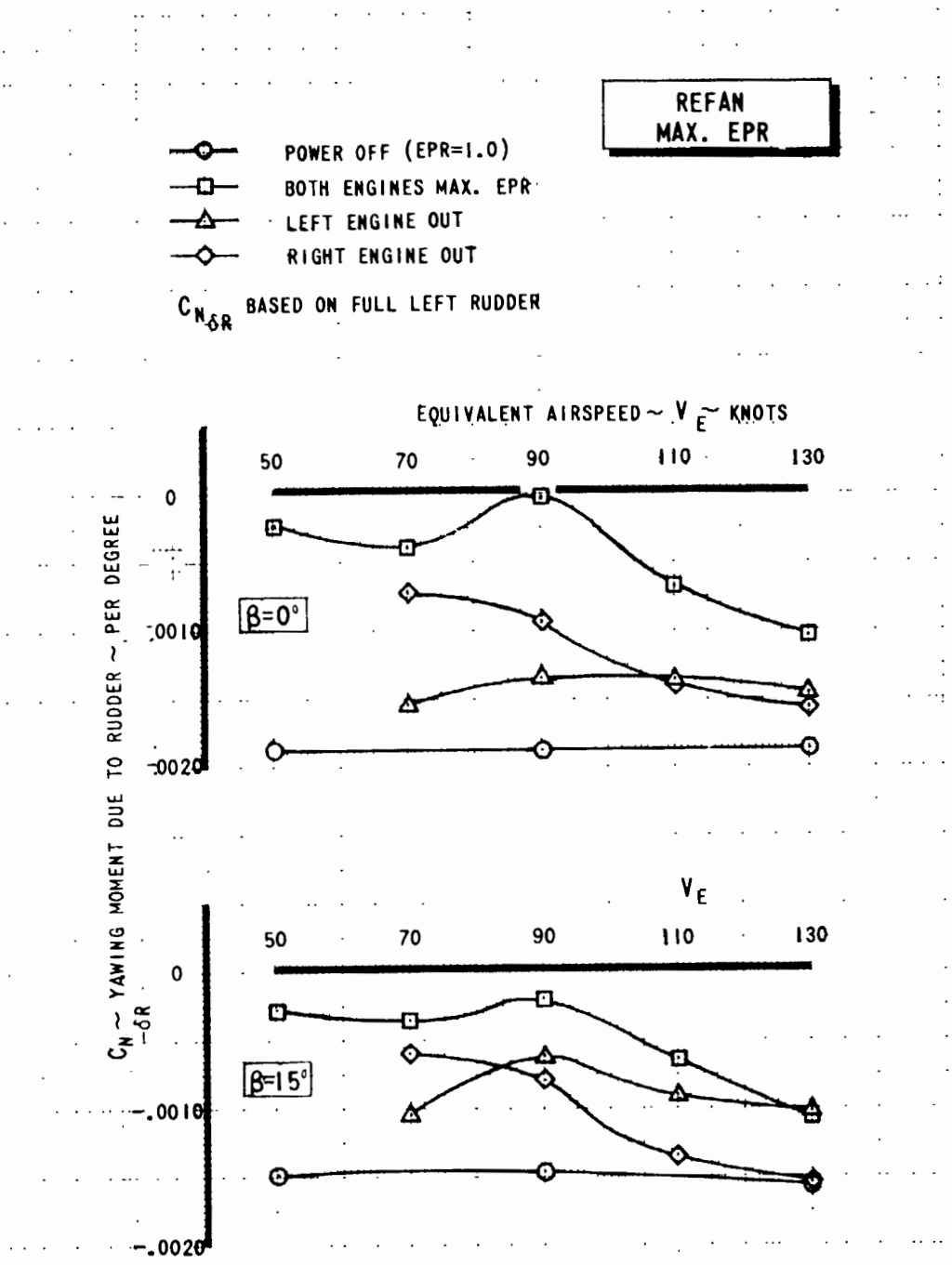

FIGURE 24.- EFFECT OF ASYMMETRIC REVERSE THRUST, REFAN AIRPLANE, MAX. EPR

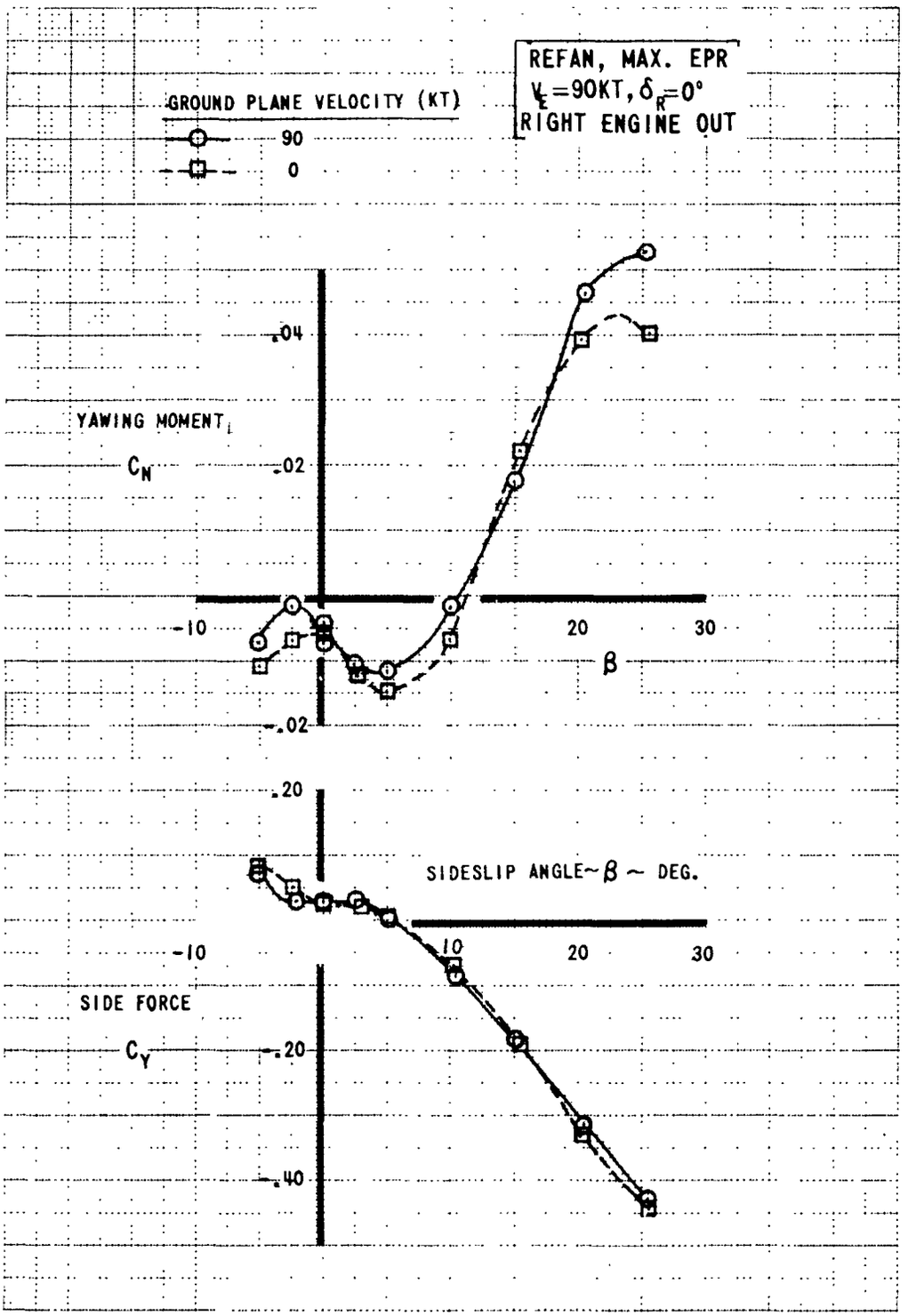

FIGURE 25.- EFFECT OF GROUND PLANE VELOCITY, REFAN AIRPLANE, MAX. EPR, V_E= 90 KT. (46.4 m/sec.), RIGHT ENGINE OUT

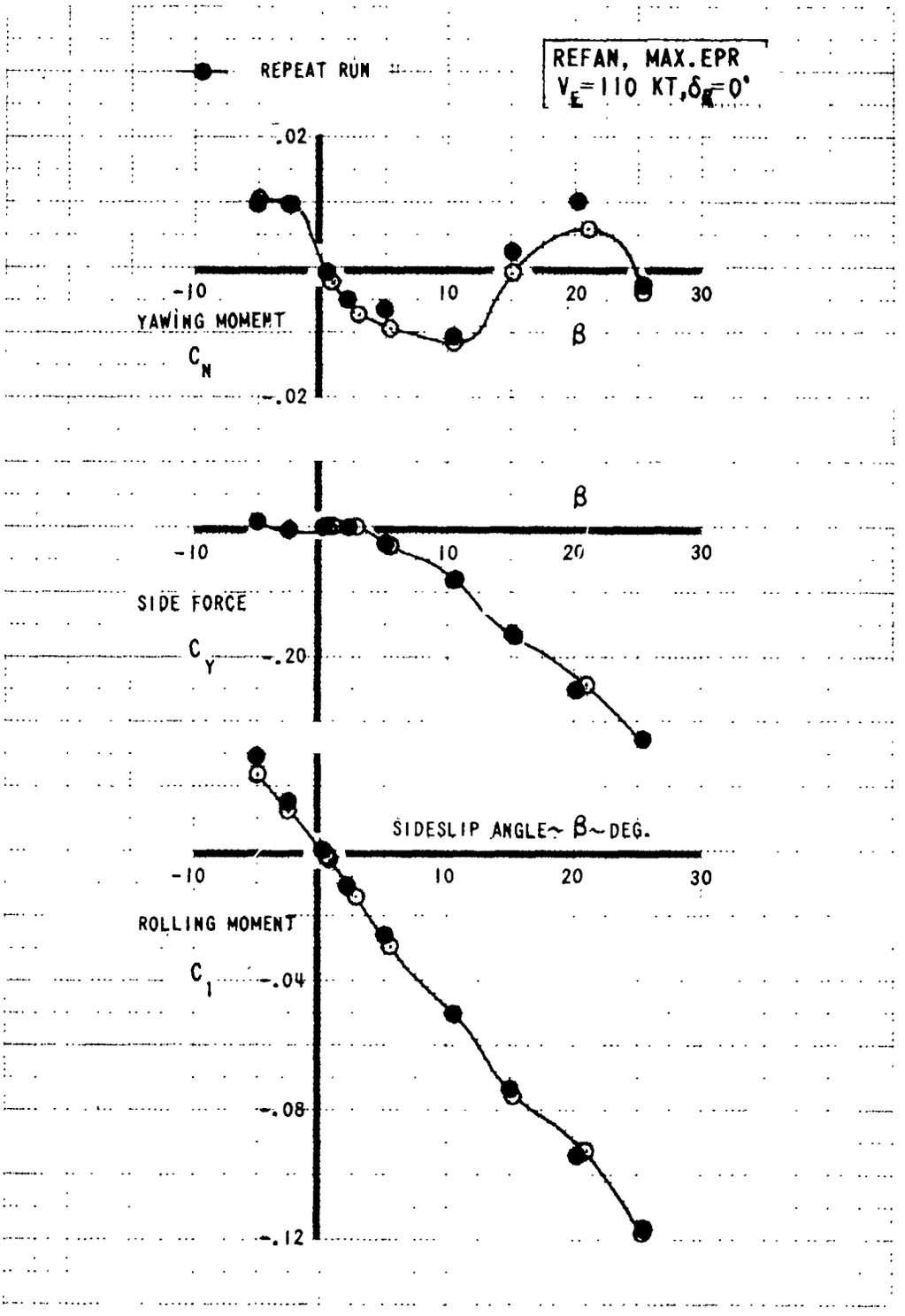

FIGURE 26.- DATA REPEATABILITY, REFAN AIRPLANE, MAX. EPR, V_E= 110 KT. (56.6 m/sec.)